2D coordination polymers: Design guidelines and materials perspective

Cite as: Appl. Phys. Rev. **6**, 041311 (2019); https://doi.org/10.1063/1.5110895
Submitted: 21 May 2019 . Accepted: 15 October 2019 . Published Online: 18 November 2019

Michael Tran, Katelyn Kline, Ying Qin, Yuxia Shen, Matthew D. Green, and Sefaattin Tongay

Applied Physics Reviews REVIEW scitation.org/journal/are

2D coordination polymers: Design guidelines and materials perspective

Cite as: Appl. Phys. Rev. 6, 041311 (2019); doi: 10.1063/1.5110895
Submitted: 21 May 2019 · Accepted: 15 October 2019 ·
Published Online: 18 November 2019

View Online Export Citation CrossMark

Michael Tran, Katelyn Kline, Ying Qin, Yuxia Shen, Matthew D. Green,[a] and Sefaattin Tongay[a]

AFFILIATIONS

School for Engineering of Matter, Transport and Energy, Arizona State University, Tempe, Arizona 85287, USA

[a]Authors to whom correspondence should be addressed: mdgreen8@asu.edu and Sefaattin.tongay@asu.edu

ABSTRACT

The advent of two-dimensional (2D) organic/inorganic layered and monolayer materials has ushered in an explosion of research to understand the synthesis, underlying physics, and exciting material properties of these materials. The field to date has produced preliminary design rules related to feasible synthesis routes that can be used to design 2D materials with a range of organic ligands and metal linkers. This review seeks to extend these design rules to predict which ligands and metals can be combined, and in what fashion, to control the thermal, mechanical, magnetic, and optoelectronic properties. Furthermore, we review the various synthetic techniques and how these can be modified to enable scalable manufacturing of 2D polymers and materials, and how this highlights the need for defect engineering and advanced characterization capabilities within the field. We conclude by discussing how together these design rules, manufacturing considerations, and characterization tools coalesce to enable new materials, applications, and fundamental insights. Particular emphasis is given to magnetism, electrical properties, and optics. Overall, this review serves as a roadmap and framework for identifying new and exciting material targets, strategies for engineering desirable properties, and conduits to streamline the manufacturing and processing of these exciting materials.

TABLE OF CONTENTS

I. INTRODUCTION

The discovery of graphene led to a new field of research in organic/inorganic chemistry and materials science dedicated to synthesizing and characterizing two-dimensional (2D) materials.[1] 2D

material systems of either inorganic or organic families have garnered tremendous research interest. Inorganic 2D materials such as transition-metal dichalcogenides (TMDs),[2] hexagonal boron nitride (h-BN),[3] MXenes,[4–8] and layered perovskites[9] have demonstrated exotic quantum properties for applications in optoelectronics, energy harvesting materials, flexible electronics, spintronics, luminescence devices, and sensors. However, these materials lack flexibility in their structural chemical design and porous behavior when compared to their polymeric counterparts. Extensive research is being done on synthetic 2D polymers for their unique material properties and rational synthesis methods. A 2D polymer is defined as a topologically planar molecular sheet made up of linked, repeating units of building blocks/monomers that extend across two dimensions. In some cases, the 2D definition also includes a few layers of stacked 2D sheets interacting through weak van der Waals (vdW) forces.[10] From a physical perspective, their ultrathin nature often means that quantum electron confinement effects are much more prominent, which gives rise to many novel optical, electronic, thermal, and magnetic phenomena.[11]

Under the 2D polymer umbrella, 2D coordination polymers (CPs) are one of the subclasses of organic materials constructed by tiling organic ligands with metal ions in the two-dimensional landscape. In the literature, these 2D CPs are also commonly referred to as 2D metal-organic frameworks (2D MOFs), coordination nanosheets (CONASHs), and even metal-organic layers (MOLs). Both 2D CPs and covalently bonded organic polymers can be selectively synthesized with defined and tunable chemical functionalities to have a variety of diverse material properties. 2D CP networks are essentially the product of Lewis acid-base pairs in which the organic ligands are bonded to a central metal ion through coordinate covalent bonds. In comparison to strictly covalently bonded 2D polymers, the insertion of a metal linker into the organic framework allows for π-d orbital interactions to contain unique electronic, magnetic, and optical properties. The weak and reversible interactions of coordination bonds of 2D CPs also allow for the self-assembly of the organic ligands and metal linkers.[10,12,13] Similar to the design flexibility offered by LEGO® building blocks, there are nearly an infinite number of combinations of organic ligands with interchangeable anchor sites, metal linkers, and clusters. This means that an unlimited number of 2D CPs can be constructed at will with different and tailorable chemical structures, physical properties, and application performances. The noncovalent reversible bonding nature of CPs also enables self-healing properties, which can enable defect-free crystalline structures.[14]

Considering the existing review articles on the chemistry of 2D CPs, this perspective article will tightly focus on the manufacturing aspects as well as novel physical properties to motivate the community to think more toward the fundamentals, manufacturing, and applications of these unique material systems. As such, we will refer to existing reviews in the literature on the chemistry of 2D CPs, but for the sake of completeness we will briefly introduce existing synthesis techniques available in the literature. The review article is arranged in a way that starts by giving proper context on synthesis and characterization of these materials (Secs. II and III) and follows up with a comprehensive discussion on how material design (ligand, metal linker, anchor site) influences the overall properties and application notes (Sec. IV). Finally, we offer our humble perspective on a number of manufacturing challenges, potentially exciting directions, and new application areas in Sec. V. While many researchers in this field have contributed to the common knowledge of 2D CPs, understandably it was virtually impossible to refer to all these great articles. For this, we offer our sincere apologies in advance.

II. SYNTHESIS AND MANUFACTURING OF 2D CPS

Preparation methods of 2D CPs have garnered a great deal of interest in the past decade. In this section, the main synthesis techniques used for both monolayer and stacked sheets of CPs (vdW CPs) will be introduced and discussed. Here, we note that there are a number of review articles, such as by Cao *et al.* and Zhao *et al.*, that provide greater details of the methods as well as dozens of examples of the synthesized 2D CPs.[15–17] Considering these existing reviews, the focus of this review will be given to those methods that have emerged over the years as champions in terms of manufacturability and compatibility with the industry as summarized in Fig. 1.

A. Bottom-up approach

Bottom-up synthesis methods directly synthesize the 2D CP sheets from metal ions and organic ligands through the self-assembling nature of the building block units (the bottom up techniques are summarized in Table I). This approach allows for easier structural and functional modification, segmented assemblies, and larger lateral dimensions. Common bottom-up synthesis methods utilize (i) liquid/liquid, (ii) liquid/solid, or (iii) gas/liquid interfaces so the growth will be physically confined to two dimensions.

1. Liquid/liquid interface

In a liquid-liquid interfacial synthesis, an aqueous solution of the metal salt is deposited on an organic solution containing the ligand. Then, the ligands and metal ions undergo coordination reactions at the interface of the two immiscible solutions, producing a suspended thin film [Fig. 1(a)]. The film can be extracted onto a substrate or filtered out. Chen *et al.* fabricated Ag and Au benzenehexathiol (BHT) 2D CPs by a liquid-liquid interfacial reaction in an aqueous sodium hydroxide solution and a co-solvent mixture of acetonitrile and ethyl acetate.[18] Silicon/silicon dioxide substrates were placed into the solution and the film was deposited as the solvent and was aspirated. The synthesis produced 276 nm thick Au-BHT films and 324 nm thick Ag-BHT films with lateral sizes up to 100 μm. This method can produce larger lateral films than the gas/liquid interfacial methods but tend to have an increased thickness due to diffusion and mixing at the interface.

2. Gas/liquid interface

In a typical gas/liquid interfacial synthesis, a thin layer of organic solution containing the ligand is spread onto an aqueous solution containing the metal salt. As the organic solvent is evaporated, the metal ion and organic ligand are confined to form coordination bonds at the interface, yielding the 2D CP [Fig. 1(b)]. The 2D film can be picked up by a substrate in a lift-up method. The Langmuir-Blodgett film technique is also popular as it allows for the CP thickness and orientation to be controlled mechanically.[17] In this case, the CP sheet(s) can be prepared by slowly compressing the solvent to form the film [Fig. 1(c)]. The 2D CP is then transferred from the liquid-gas interface onto a solid substrate. Makiura and Konovalov demonstrated this process with the reaction between tetra-pyridyl-porphyrin zinc (Zn-TPyP) in a mixed chloroform-methanol solvent and Cu ions in water within a

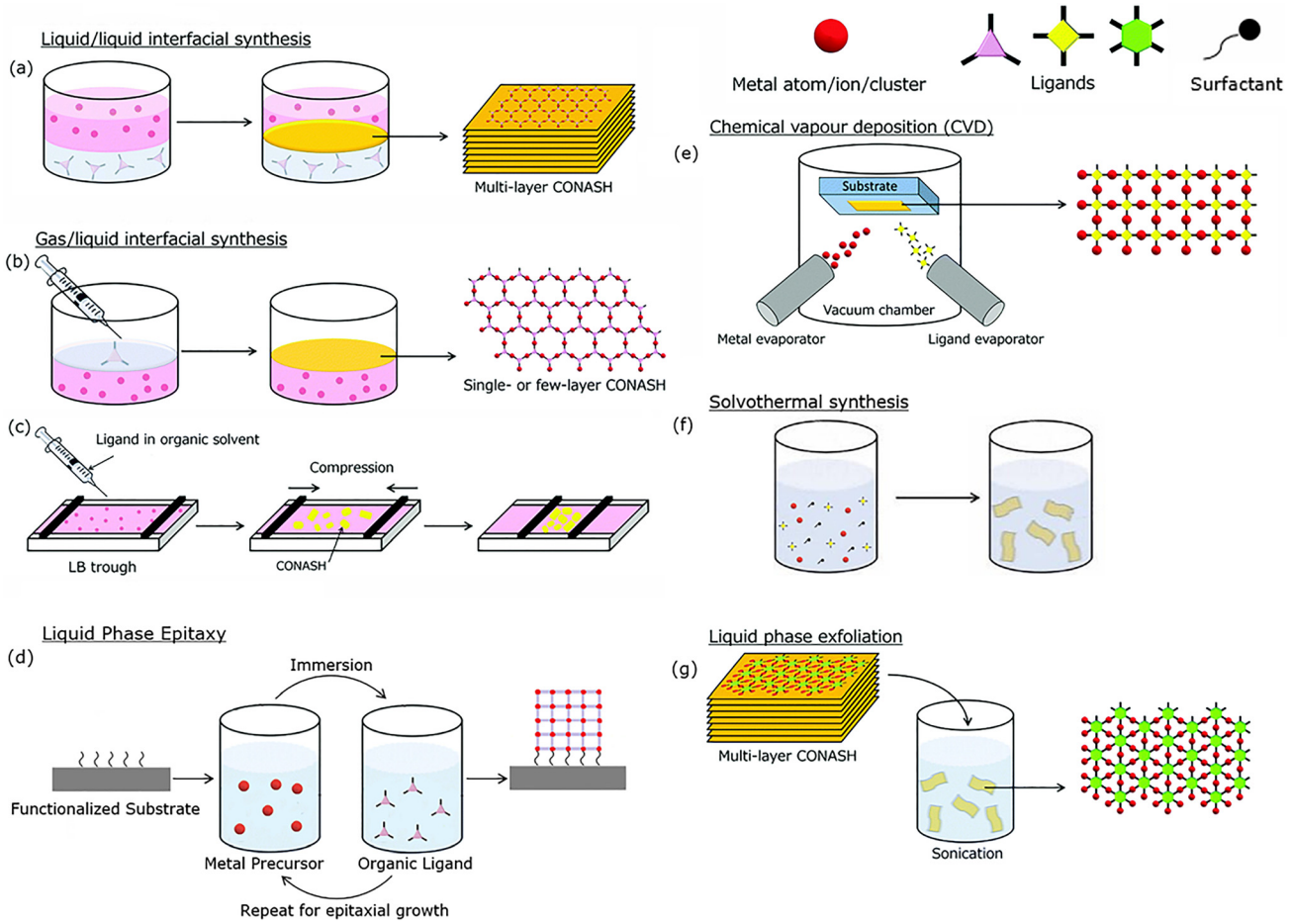

FIG. 1. Schematic illustrations of (a) liquid/liquid interfacial synthesis, (b) and (c) gas/liquid interfacial synthesis,[24] (d) liquid phase epitaxy (solid/liquid interface),[25] (e) CVD synthesis,[24] (f) solvothermal synthesis, and (g) liquid-phase exfoliation.[24] Adapted with permission from Sakamoto *et al.*, Chem. Commun. **53**, 5781 (2017). Copyright 2017 Royal Society of Chemistry.

Langmuir trough.[19] The carefully controlled surface pressure of the trough produced molecularly thin sheets with domain sizes of approximately 410 nm. The gas/liquid interfacial synthesis has successfully formed many monolayer and stacked sheet CPs.[19–21]

3. Solid/liquid interface

A more recent synthetic approach is liquid phase epitaxy, which involves the solid-liquid interface. Epitaxial growth of 2D CPs requires flat substrates functionalized by surfactant molecules. The functionalized substrate becomes a template for fabricating self-assembled monolayers (SAMs). This method involves the use of surfactant molecules that can self-adhere as a monolayer onto a metal/metal-oxide substrate with the free functional groups serving as the nucleation sites for coordination polymer assembly. An example includes functionalizing metal substrates with thiol molecules or hydroxyl molecules that will be used as a nucleation-directing template. Gu *et al.* offers an extensive review on various established epitaxial growth techniques of

TABLE I. Pros and cons of common bottom-up growth techniques.

Methods	Pros	Cons
Gas/liquid interface	Monolayer thickness	Small domain sizes
Liquid/liquid interface	Larger domain sizes	Larger thickness
Solid/liquid interface	Thickness and orientation control	Functionalized to substrate
CVD	Thickness control, high crystallinity	Small domain sizes, functionalized to substrate
Solvothermal	Manufacturing scalable	Thickness control is more complex

2D CPs.[22,23] The most common and flexible method involves the dipping layer by layer method, wherein the SAM undergoes an alternating sequence of simple immersion processes into solutions containing either the metal ion or organic ligands.[24,25] The self-assembly of the CPs will occur layer by layer on the functionalized substrate with each immersion into the solution. Recently, Wang and co-workers developed a layer-by-layer epitaxial growth protocol to synthesize 2D zinc tetracarboxylate-porphyrins (TCPP) for solar cell applications.[23] The group started with a fluorine-doped tin oxide substrate (FTO) functionalized with hydroxyl groups. Similar to the process shown in Fig. 1(d), the aforementioned procedure involved cyclic immersions of the FTO substrate into a zinc acetate solution, then ethanol, then a porphyrin solution, and then ethanol again. The thickness was controlled from a single layer to 200 nm by controlling the number of immersion cycles. The FTO with thin film Zn-TCPP was then directly integrated into a dye sensitized solar cell. Epitaxial growth allows for increased orientation and thickness control, although the material properties will be affected by the substrate and chemical functionalization.

4. Chemical vapor deposition

CVD has been utilized to synthesize other 2D materials and has also been adapted to prepare 2D CPs. The CVD process is carried out under ultrahigh vacuum such that metal precursors and ligand molecules are evaporated toward a metal substrate [e.g., Cu(100), Au(111), and Ag(111)].[16] This is followed by thermal annealing to crystallize the nanosheets. The parameters that control the thickness and crystallinity of the 2D CPs include substrate temperature, evaporation rates of precursors, and annealing temperature. In 2016, Wurster *et al.* synthesized 2D tetra-phenyl-porphyrins (TPyP) with Fe and Co metal linkers on Au(111) substrates.[26] The process involved the sublimation of the TPyP ligand onto the substrate followed by evaporation of atomic iron and cobalt using an electron beam evaporator. Scanning tunneling microscopy (STM) confirmed a uniform monolayer thickness across the substrate. Characterization of the bimetallic sheet on the Au(111) electrode showed outstanding overpotentials and turnover frequencies for water oxidation catalysis. Atomic layer deposition (ALD) is another vapor-phase growth method that has been traditionally employed for 3D coordination polymer preparation.[27–29] Various saturated precursor vapors are pulsed to the main reaction chamber with an inert carrier gas and are deposited onto the hot wafer substrate inside to kick off interfacial reactions. Given the absence of out-of-plane interactions in 2D CPs, this method could potentially provide atomic monolayer-precise growth.

5. Solvothermal growth

A promising synthesis method in terms of manufacturing is in-solution phase synthesis in which 2D CPs can be self-assembled in a one pot solution. From this reaction, colloidal suspensions or precipitates of the 2D CPs are produced and can be extracted via centrifugation or vacuum filtration.[30,31] One-pot reactions can be performed under a variety of conditions including solvothermal, hydrothermal, and surfactant assisted methods. Solvothermal reactions involve high temperature growth of crystals from a nonaqueous solution while hydrothermal processes are carried out in an aqueous environment.[32–35] Surfactants and modulators are typically utilized to control the thickness and number of layers. These added molecules bind to the surfaces of the growing sheets to prevent stacking and reduce the surface energy, confining the material into ultrathin sheets. Generally, the supersaturation of surfactants can result in thinner sheets. However, this procedure often requires subsequent exfoliation of the precipitate after initial synthesis to achieve few to single layer thicknesses. Exfoliation will be discussed briefly in the Sec. II B. Zhou *et al.* demonstrated the synthesis of 2D CPs by solvothermal methods with coronene and planar iron-bis(dithiolene) as metal linkers.[36] The reaction occurred in a sealed vial with a mixture of N,N-dimethylformamide (DMF) and water heated to 120 °C for 48 h to produce micrometer-sized crystals. In a surfactant-assisted experiment, Cao and co-workers synthesized self-supporting 2D CPs through a solvothermal reaction.[37] The reaction occurred between Zr_6 and $[Hf_6O_4(OH)_4(HCO_2)_6(\text{carboxylate})_6]$ with benzene-1,3,5-tribenzoate ligands in a mixture of DMF, formic acid, and water at 120 °C. The formate groups from the acid capped the z-directional bonding of the ligands to encourage planar growth. Varying the concentration of Hf clusters and formic acid led to the controllable tuning of the nanosheet thickness from bulk crystals to monolayers. In general, one-pot solution-phase synthesis is more scalable than interfacial synthesis and therefore would be the preferred method for commercial manufacturing. However, there are still many challenges in synthesizing highly crystalline monolayers to ultrathin sheets with large lateral dimensions.

B. Top-down techniques

In contrast to bottom-up techniques, this method starts with bulk vdW crystalline materials containing 2D stacked layers held together by weak interlaminar forces. Individual monolayers are isolated by mechanical exfoliation or by a liquid delamination process. While micromechanical exfoliation is one of the most popular top-down approaches for 2D materials, generally liquid phase exfoliation (LPE) first comes to mind among top-down methods of 2D CPs. LPE involves ultrasonication to delaminate larger 2D crystals/powders in solvent and produce a colloidal suspension of the sheets [Fig. 1(e)].[38–42] LPE can be further manipulated by crystal-solvent chemistry to control the exfoliation process. In general, the surface energies of the solvent and sheets should match to encourage exfoliation and stabilization of the suspended sheets. An example is the use of water or alcohol to delaminate 2D CPs held together by interlayer hydrogen bonds.[17] Recently, Mukhopadhyay and co-workers exfoliated layered CPs consisting of 2,2-diphenylbenzopyran ligand backbones with pyridyl/carboxylate functionalities and Cd/Zn linkers.[43] The bulk powders were first synthesized through solvothermal conditions, forming layered CPs with pores occupied by solvent molecules. Due to the hydrophilic nature of the carboxylate functionalities, LPE was performed in ethanolic solutions. The LPE proceeded for 30 min and produced 3–6 nm thick sheets with lateral sizes around 500 nm.

III. CHARACTERIZATION

It is necessary to study the crystallinity, structure, molecular arrangements, and orientation in 2D CPs at nanoscale dimensions to understand the interrelationship between material properties and synthesis methods. In general, multiple characterization techniques are required to fully investigate the material properties. We will briefly introduce several advanced characterization techniques that are used to probe the structural and electronic information of 2D CPs.

A. X-ray diffraction

X-ray diffraction is a common method to identify the crystal structure and periodicity of 2D materials. Powder X-ray diffraction (PXRD) is typically used for powder and thicker samples, providing lattice information on the layered structure. However, this method is not as useful in characterizing thin films and few-layer sheets. Grazing incidence X-ray diffraction (GIXRD) with synchrotron radiation is recommended to obtain diffraction of ultrathin materials. This method uses small incident angles for incoming X-rays to limit penetration and encourage diffraction at the surface. Huang and co-workers demonstrated GIXRD characterization on a 60 nm thin nanosheet to determine the interlayer distance and crystal lattice structure that matched theoretical predictions.[44]

B. X-ray photoelectron spectroscopy

X-ray photoelectron spectroscopy (XPS) is a technique that probes the chemical composition and bonding environment. This method analyzes the energy of the photoemitted electron at the surface, making it suitable for 2D CPs with nanoscale thicknesses. For example, XPS was utilized by Lahiri and co-workers to confirm the composition of a 2D nickel hexaaminobenzene (HAB) CP.[45] The scan confirmed the presence of all the involved elements (C, N, and Ni) as well as the oxidation state of the Ni in the complex.

C. Atomic force microscopy

Atomic force microscopy (AFM) remains the standard technique in characterizing the thickness and quantifying the number of atomic layers of many 2D materials. This method measures the height of the material on a flat substrate from the intermolecular force between the probe tip and sample surface. By manipulating the AFM thickness measurements with the predicted molecular sheet thickness, one can determine the quantity of sheets in the sample.

D. Scanning tunneling microscopy

Scanning tunneling microscopy (STM) is used to image surfaces at an atomic scale. This method can probe individual atoms based on the local density of states on the surface of the sample based on the principle of quantum tunneling. Kumar and co-workers applied STM characterization to a 2D CP consisting of dicyanobiphenyl (DCBP)/dicyanoanthracene (DCA) ligands with cobalt metal linkers grown on weakly interacting substrates such as graphene.[46] Their work showed clear images of the 2D CP's honeycomb periodicity (Fig. 2). From the STM images, the coordination bond lengths and lattice constants were extracted. The group combined additional scanning tunneling spectroscopy data with density functional theory (DFT) calculations to investigate the intrinsic electronic properties and band structure of the 2D CP.

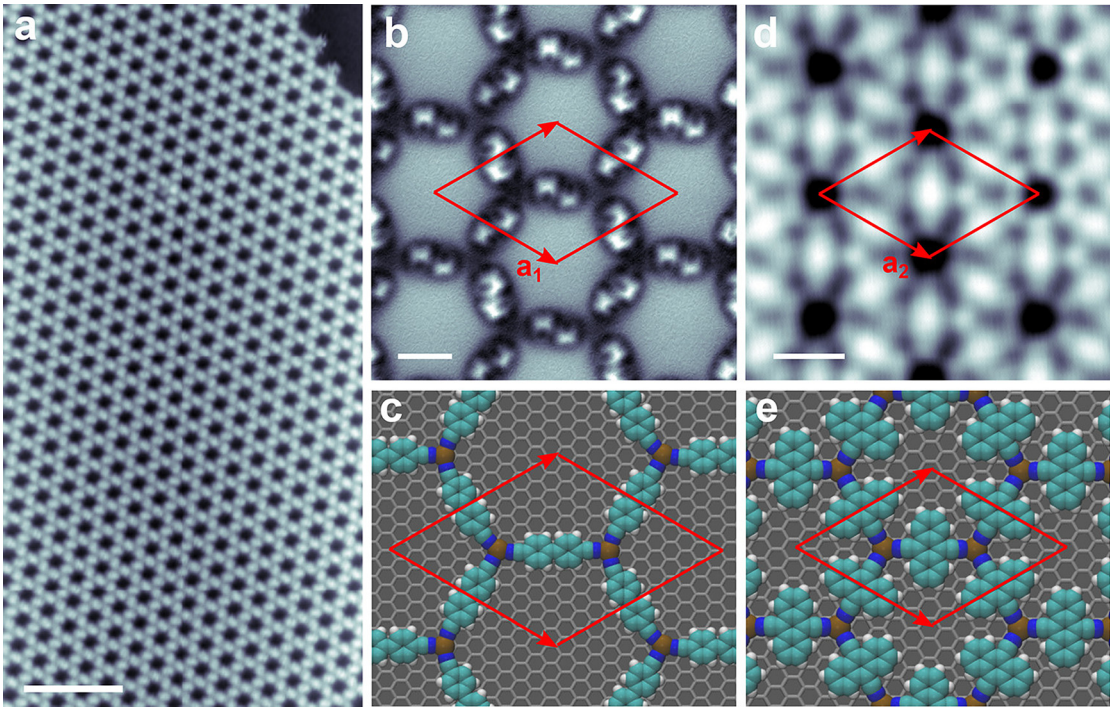

FIG. 2. Overview of two MOFs. (a) An STM overview image of a honeycomb $DCBP_3Co_2$ MOF on a G/Ir(111) surface. The scale bar is 10 nm. Imaging parameters: 1.23 V and 3.3 pA. (b) Constant height frequency-shift, Δf, nc-AFM image of $DCBP_3Co_2$ MOF acquired with a CO-terminated tip. The scale bar is 1 nm. (c) DFT-simulated structure of the $DCBP_3Co_2$ MOF on graphene. (d) STM topography image of the DCA_3Co_2 MOF. The scale bar is 1 nm. Imaging parameters: −1 V, 15 pA. (e) DFT simulated structure of the DCA_3Co_2 MOF on graphene. Red parallelograms indicate the unit cells. Reproduced with permission from Kumar *et al.*, Nano Letters **18**, 5596–5602 (2018). Copyright 2018 American Chemical Society.

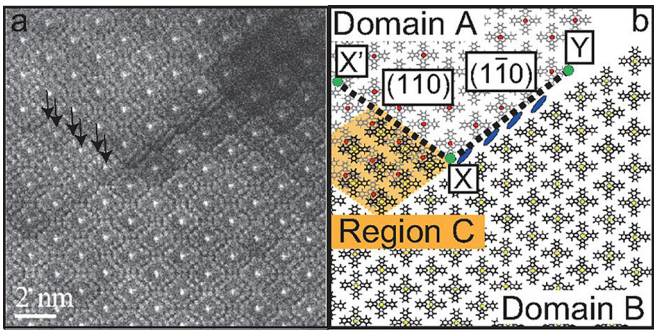

FIG. 3. (a) LAADF-STEM image of the complex defect region. The stacking fault was observed along the plane and Cl16CuPc molecules with irregular orientation were identified in the grain boundary along the plane as a line contrast. (b) Schematic diagram of molecular columns corresponding to (a). The two domains, A and B, can be seen as gray and black molecules, and molecules along the XY grain boundary are shown as blue ellipses. Reprinted with permission from M. Haruta and H. Kurata, "Direct observation of crystal defects in an organic molecular crystals of copper hexachlorophthalocyanine by STEM-EELS," Sci. Rep. **2**, 252 (2002). Copyright 2002 Springer Nature.

E. Transmission electron microscopy

High-resolution transmission electron microscopy (HRTEM) can provide images of the lattice edges of the metal linker groups. Although not impossible, the lighter elements of C and N are much more difficult to visualize through traditional HRTEM methods. Another concern with electron microscopy is electron irradiation damage to the sample. A low electron dose and/or cryotechniques are necessary to preserve the integrity of the material. Haruta and Kurata demonstrated the use of low angle annular dark-field scanning transmission electron microscopy (LAADF-STEM) to directly observe defects at atomic resolution of a copper hexachlorophthalocyanine thin film.[47] By utilizing a low electron dose and optimized detection angles, the technique resolved clear contrast of the light elements (C and N) along with the heavy elements (Cl and Cu). The images provided information on molecular orientation and identified stacking faults in the grain boundaries (Fig. 3).

IV. DESIGN AND PROPERTIES

The organic ligand, the anchorage sites, and the central metal linker repeat to form the polymeric structure (Fig. 4). Due to the unlimited combinations of organic ligands, metal linkers, and attached functional groups, 2D CPs can possess a wide range of material properties. The choice of material, design and structure, and synthetic conditions will have a significant impact on the material's structure and properties.[42,48] Here, we will briefly review the important parameters when designing 2D CPs and highlight recent trends observed that prove useful for tailoring specific properties.

The geometry of the coordination bond between metals and ligands is crucial in determining the material's final dimensionality and properties. The most common coordination geometry for 2D planar CPs is square planar with bidentate anchorage sites of two ligands onto a metal linker. There have also been a few cases of monodentate coordination bonds. A sheet can also be designed in a trigonal planar geometry with anchorage sites of three ligands. These can produce periodic arrays of square or honeycomb (hexagonal) lattices.[46,49,50] The hexagonal lattice is intriguing due to its analogous structure to graphene. There are also a few reports on materials with the Kagome lattices.[51,52] This lattice consists of a hexagonal pattern with equilateral triangles arranged so each hexagon is surrounded by the triangles and can provide novel properties due to its unique symmetry.

A. Ligands and control of geometry

There are a wide variety of organic ligands that can be used to synthesize 2D CPs. Ligands can be chosen for their charge (neutral or anionic), length and flexibility, donor atoms (O, N, or S), density of conjugation (π bonds), and functionality (hydrophilicity, bonding sites, catalysis, etc.). The backbones for 2D CPs are aromatic compounds due to their high stability and conjugation with attached functional groups that form the coordination link. The high density of electrons and pi-bonds can provide unique electronic and optical properties. Their constricted rotational nature also serves to restrict out of plane growth. For example, phthalocyanine-,[50,53–59] porphyrin-,[19,23,50,60–65] and benzene-derived[24,45,66–71] ligands are prime examples of short ligands with a high density of conjugated bonds that allow for efficient metal interaction pathways and π-d conjugation. Much research is being conducted on these base materials for their potential catalytic, optoelectronic, and magnetic properties. Functional groups of pseudohalides, which are short bridging ligands such as cyanides, azides, and nitrile donors, can provide predictable binding modes that prevent out of plane rotation while their short bridges provide excellent magnetic/electronic exchange.[71] The carboxylic acid ligands produce very strong

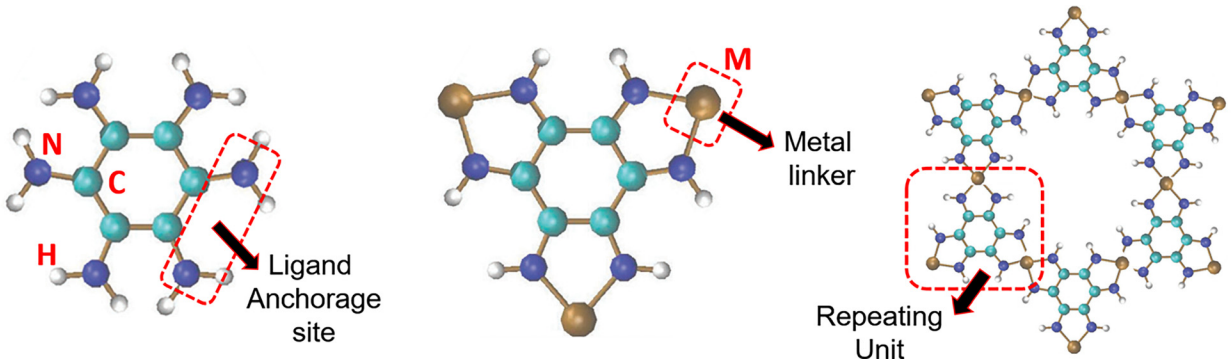

FIG. 4. Schematic diagram of 2D CP building blocks.

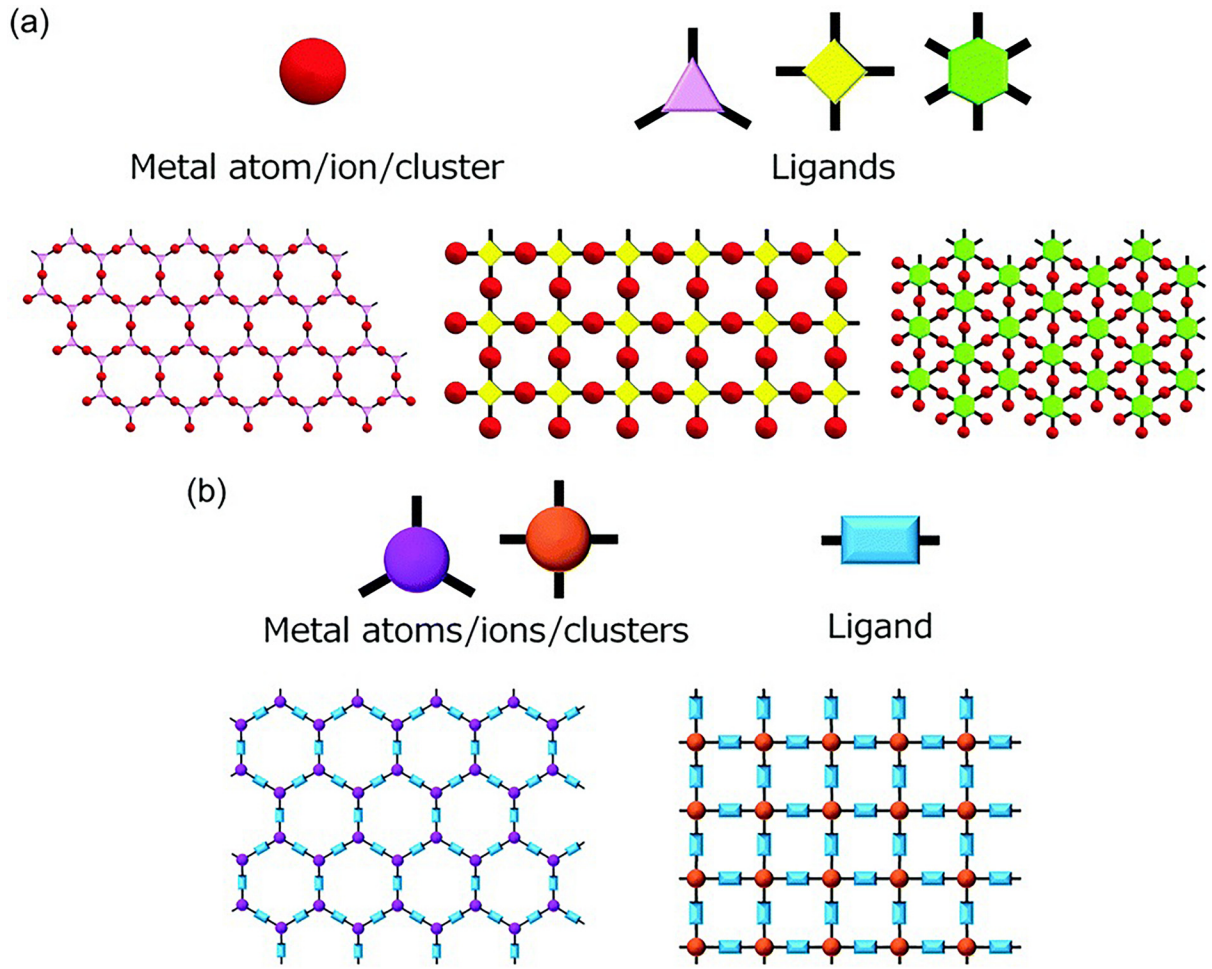

FIG. 5. Schematic illustration of (a) a metal atom, ion/cluster, organic ligand molecules with three-, four-, sixfold symmetry, (b) metal atoms/ions/clusters with three- and fourfold coordination symmetry and a linear bridging ligand.[72] Reproduced with permission from Sakamoto *et al.*, Chem. Commun. **53**, 5781 (2017). Copyright 2017, Royal Society of Chemistry.

bonds and can be incorporated into coordination polymers easily due to their ability to bind in a monodentate or bidentate fashion. Other common organic functionalities include pyridyls, azoles, and thiols. More complicated ligands (e.g., those with multiple organic anchorage groups) can be used to create mixed organic ligands to utilize multiple/mixed properties of more than one bridging ligand.

The ligands and metal ions are chosen to encourage planar geometry combinations, as shown in Fig. 5. These ligands will be selected to form 2, 3, or 4 coordination sites to the metal linker. For example, benzene is a conjugated six carbon ring that can hold up to six functional groups. An illustration of hexaaminobenzene (HAB) is shown in Fig. 6(a). Due to the steric proximity, the amines will form

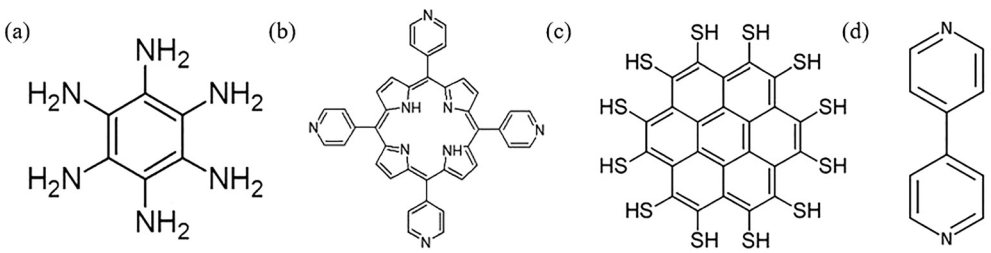

FIG. 6. Illustration of (a) HAB, (b) TPyP, (c) PTC, and (d) bpy.

bidentate anchorages to a metal linker to realize a total of three coordination sites. This results in the hexagonal lattice of the threefold symmetry shown in Fig. 5(a).[45] Tetra-pyridyl-porphyrin (TPyP) contains four possible coordination sites in the outer pyridyl groups [Fig. 6(b)]. This ligand coordinates with a metal linker to form a square planar lattice, similar to the fourfold symmetry geometry of Fig. 5(a).[73] 1, 2, 3, 4, 5, 6, 7, 8, 9, 10, 11, 12-perthiolated coronene (PTC) with 12 thiol functional groups is displayed in Fig. 6(c). Due to steric hindrance, the two sulfurs on each side of the benzenes will form a bidentate bond with a metal linker. This will result in six coordination sites to form the sixfold symmetry with hexagonal periodicity of Fig. 5(a).[36] Bipyridine (bpy) in Fig. 6(d) has two coordination sites possible. It will most likely form the fourfold coordination symmetry, resulting in a square planar structure.[74]

1. Relation to separation properties

In separation applications, the 2D membranes are typically multilayered and porous, allowing them to achieve separation through either size selectivity (controlled by the pore size and geometry) or chemical absorption (controlled by chemical functional groups). The pore configuration and pore size need to be considered to increase the number of active sites and to control molecular separation. Short bridging ligands are a good way to restrict pore sizes, although longer ligands can create smaller pores with increasing interpenetration of 2D polymer sheets. Interpenetration involves the folding of the 2D sheets into each other instead of lying within its own plane. Increasing interpenetration consequently will decrease the pore sizes. Flexible ligands are also more likely to produce interpenetrated sheets than rigid ligands since they contain more rotational freedom. Hijikata *et al.* synthesized four 2D CPs with varying dinitrogen linkers; 1,4-diazabicyclo[2,2,2]octane (dabco), 1,4-bis(4-pyridyl)benzene (bpb), 3,6-bis(4-pyridyl)-1,2,4,5-tetrazine (bpt), and 4,4′-bipyridyl (bpy) with Zn^{2+} metal centers.[75] Density functional theory calculations showed that the length of the organic ligands dominated the stacked assembled structures and flexibility. The shorter ligands (dabco, bpb, and bpt) lacked any interpenetration, while the longest ligand (bpy) showed interpenetrated sheets. Consequently, the shortest ligand (dabco) had the smaller pore size of the first 3 ligands but the longest bpy ligand was measured to have the smallest pore size due to its interpenetrated structure.

The effectiveness of chemical and gas adsorption can be selectively tuned by incorporating specific functional groups into the organic ligands. The free functional groups that are not used in the coordination bonds can capture targeted molecules through either physisorption or chemisorption. Yan *et al.* synthesized layered 2D CPs with 5-aminotetrazole and Zn^{2+} for CO_2 capture applications.[76] Aminotetrazole's coordination chemistry involves the nucleophilic nitrogen atoms in the ring, leaving a free amine group. This ligand was chosen because the free amino groups are excellent for binding with CO_2 molecules and structure can accept a variety of polar guest molecules into its structure for additional functionality. Results showed high CO_2 uptakes at 1 bar and 273 K, with a maximum uptake of 2.4 mmol/g. In the same paper, they were able to attach a dicarboxylate functional group to the amine, which further enhanced CO_2 adsorption to 2.9 mmol/g and improved selectivity of CO_2 over CH_4 and N_2 (Fig. 7). Xu *et al.* compiled a short summary of gas separation performances regarding CO_2 adsorption, which revealed a majority of

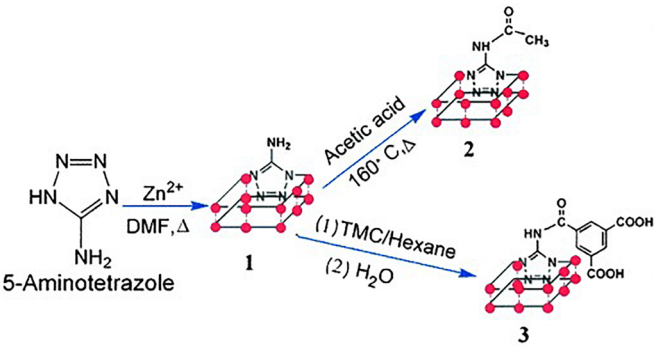

FIG. 7. Synthesis schematic of 5-aminotetrazole and Zn^{2+} for CO_2 applications.[76] Reproduced with permission from ChemPlusChem **78**, 86 (2013). Copyright 2013 John Wiley and Sons.

previously published 2D CPs containing dicarboxylate functionalities.[77] Carboxylate ligands have also proven successful in improving water filtration performance. The coordination polymer membranes were incorporated into the polyamide (PA) active layer, which caused a higher water permeability, lower salt solute flux, and increased longevity.[78] The increased hydrophilicity of carboxylates enabled a thin film of water to reduce fouling. Dai *et al.* synthesized copper benzenedicarboxylate (BDC) nanosheets and incorporated them into the PA active layer for forward osmosis applications.[70] The composite membrane demonstrated a 50% increase in water flux, 50% decrease in reverse solute flux, and a slower flux decline than the control PA layer. The increased antifouling behavior can be attributed to dicarboxylate's hydrophilicity and copper's biocidal ability.

B. Metal linker design

The most common metals used in 2D CPs are transition metals (TMs) with their unique d-block shells, including Mn, Fe, Co, Ni, Cu, Zn, Pd, Ag, Cd, and Mg.[79] Generally, the first row of transition metals (TMs) is preferred for their cost, abundance, and chemical predictability in producing metal-organic planar complexes. The oxidation states for these ions are typically 2+. Divalent metal ions usually form 4 or 6 coordinate metal centers whereas the trivalent metal ions, like In^{3+}, thermodynamically prefer to form 6 or 8 coordinate metal centers.[80] F-block lanthanide metal ions exhibit much higher coordination numbers and predominantly form 3D structures, although some nanosheets have been reported. S-block metals have a strong ionic tendency, which makes it difficult to predict the 2D CP structure and properties. Although a few 2D coordination polymers have been synthesized with these more complex metal groups, their design and properties will not be discussed in detail here.

1. Relation to catalysis

Considering their single atom status embedded into a 2D organic matrix, their potential applications are primarily related to single atom catalysis and water splitting/H_2 generation applications. These catalytic materials typically require porous structures with unsaturated metal atoms or semiconductive metal oxides.[79] Due to the planar structure of 2D CPs, the metal center is more likely to have exposed catalytic sites than their bulk counterparts. The advantages of

coordination polymer catalysts include improved catalyst recovery, enhanced stability, increased number of active sites, electrical conductivity, and shape selectivity. The applications of catalytic CPs vary widely. Many researchers have focused on CO_2 capture and conversion,[72,80,81] degradation of organic dyes,[72,82] reduction of nitrophenol,[31,81] Cr(IV) reduction,[83] and biological enzymatic applications.[83,84]

For heterogeneous catalytic processes, the unsaturated metal atoms can be integrated as the metal linker between organic groups, serving as both a structural component and an active site. Unlike 3D coordination polymers, the 2D coordination of the square planar or trigonal planar geometry allows space for reactants to adsorb onto the metal and initiate catalysis. Jia *et al.* investigated the water oxidation catalysis efficiency of 2D CPs made from Ni and phthalocyanine.[59] The thin film deposited onto FTO demonstrated efficient catalytic activity with a mass activity of 883.3 A g^{-1} and an onset voltage potential of 0.25 V, representing one of the highest oxygen evolution reaction catalytic activities among molecular catalysts. The strong activity is due to the material's high intrinsic metallic conductivity, which enabled fast electron transfer during electrochemical reactions as well as a high specific surface area.

Unsaturated metal atoms can be incorporated through guest-host interactions. In this method, the catalytic metals will be dispersed onto layered coordination polymer supports. The metal will be deposited into the pores of the stacked 2D CP as tiny nanoparticles. The metal nanoparticles can be selected for their intended reaction within the suitable framework. In one study conducted by Yan *et al.*, Au nanoparticles nucleated on the surface and between the stacked layers of a mixed-ligand layered Ni CP, which were then used to catalyze aqueous reduction reactions of nitrophenol.[33] The experiment showed that the pore size of the nanosheets dominated the conversion rate of the nitrophenol molecules. The decreased pore size and, in turn, reduced Au nanoparticle radius resulted in a higher surface area to volume ratio and increased catalytic activity. Zhang *et al.* synthesized 2D zirconium-BDC (BDC: benzenedicarboxylate) CPs with Ru nanoparticles supported on the nanosheets.[67] The Ru nanoparticles within the nanosheets realized high efficiency in the hydrogenation of levulinic acid to γ-valerolactone.

Photocatalysis involves the irradiation of light onto a semiconductor to create electron-hole pairs that can react with surface-adsorbed reactants. Efficient photocatalysis requires materials with strong light absorption, sufficient redox potential, fast charge separation, and a high carrier mobility.[85] Sakamoto *et al.* reported a study showing the difference in catalytic activity between two CP isomers, which were obtained by using two different synthesis solvents.[72] The bandgap of each isomer was determined to be 1.65 eV and 2.24 eV. Their photocatalytic activity for the degradation of organic dyes was then studied, and the CP structure with a lower bandgap exhibited greater photocatalytic degradation. To demonstrate the effectiveness of 2D photocatalytic materials, He *et al.* synthesized 2D CP nanosheets of $ZrCl_4$ and Ni-tetrakis(4-carboxyphenyl)-porphyrin.[86] Porphyrin compounds were selected due to their known efficiency in light harvesting for O_2 generation. The comparison of the stacked sheets to the bulk counterparts showed superior photocatalytic oxidation of 1,5-dihydroxynaphthalene (1,5-DHN) to synthesize juglone. The bandgap, charge mobility, and pore design will impact the efficiency of the photocatalytic material. The design of the crystalline bandgap and charge mobility will be further discussed in Sec. IV C.

C. Conjugated ligand-linker

The semiconducting properties of coordination polymers are the result of the hybrid crystalline structures consisting of insulating inorganic ligands and conducting metal linkers. Depending on the structure and components, the HOMO (highest occupied molecular orbital) and LUMO (lowest unoccupied molecular orbital) can exclusively originate from the ligand itself or from the metal-ligand interaction.[87] Depending on the material size, the HOMO and LUMO can be referenced as the valence and conduction band, respectively. The difference between the two bands is called the bandgap. The type and strength of the metal-ligand interaction can drastically alter the coordination polymer's electronic states, the band structure, and electronic characteristics.[88]

1. Relation to electronic properties

The design trend for 2D CPs based on dozens of reported literature results is shown in Fig. 8. In summary, for a given organic ligand, the electronic bandgap will generally increase as the metal linker is substituted in the following order: Cu, Ni, Mn, Co, Fe, Mg, Zn, and Cd. Less electronegative atoms of the ligand anchorage site between the metal and organic ligand will result in a larger band dispersion and a decreased bandgap. Layered materials will have a larger bandgap than defect-free 3D bulk materials. Similar to bulk materials, an increase in the density of conjugated bonds and number of aromatic rings of the organic ligands will narrow the CP's bandgap. The bandgap was also observed to generally decrease as the planar structure transitions from hexagonal to square to the Kagome lattice.

Electrical conductivity in a coordination polymer is dictated by the electronic structure, density of states, and the electronic mobility of free carriers. The behavior of free holes and electrons is generally dictated by the metal ion. Aromatic compounds are primarily used as the polymer backbone for their highest density of conjugation and resonance that allows for pi-bond charge hopping. Interestingly, a majority of recently reported materials regarding electrical conductivity in 2D CPs reveals stacked honeycomb, square planar, or Kagome lattices. These lattices consisted of conjugated aromatic-derived ligands such as benzene or triphenylene with ortho-disubstituted N, O, or S donor atoms coordinated with first row transition metals such as Cr, Mn, Fe, Co, Ni, and Cu. In a computational study, Tiana *et al.* determined that the less electronegative species of the group O, S, and N, linking atoms generally decreased the bandgap and increased the band dispersions of 1D polymer chains.[89] The weaker electronegativities of S compared to N and O equate to more electronic orbital overlap and improved electron delocalization. Replacing the linking functional groups in copper and hexa-(hydroxy to amino to thiol)-benzene decreased the bandgap.

Single layer sheets possess unique electronic properties when compared to stacked, multilayered sheets. Bulk 2D CPs experience interlayer van der Waals or pi-pi interactions that can significantly alter the electronic properties from the monolayer polymer. A trend has been observed in 2D CPs, going from a single layer to a few layers and to bulk, that the conductivity and metallic behavior increase, in the absence of defects. Chen *et al.* predicted, using DFT calculations, that a single $Ni_3(HITP)_2$ sheet is a semiconductor with a narrow bandgap while the multilayered calculations showed a metallic band structure.[51] In another study, Clough and co-workers demonstrated

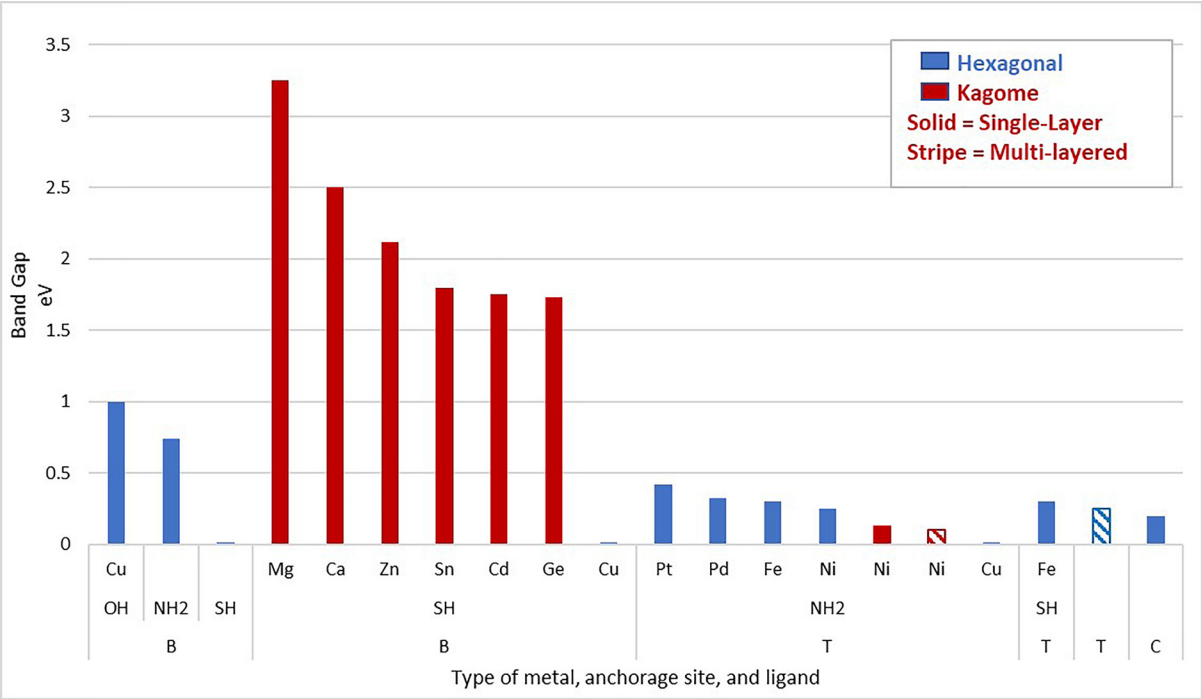

FIG. 8. Observed trends in the bandgap based on the choice of metal linker, anchorage site, organic linker, lattice structure, and thickness (B: benzene, T: triphenylene, C: coronene).[89–96]

decreasing resistivity as the film thickness increased from 10 nm to 50 nm for 2D Co hexahydroxytriphenylene.[90]

Transition metals can be varied to tune the electronic properties of 2D CPs. The band structure will heavily depend on the interaction between the organic ligand's p-orbitals and the transition metal's outer electrons, particularly the d-orbitals. Density functional theory calculations have been a useful method to investigate the band structure of 2D CPs. Sun *et al.* provided an experimental and computational study on coordination polymers and the tuning of the bandgap through varying the metal linker.[91] They found that the electrical conductivity generally increased, and the bandgap decreased from high spin Fe^{2+}, Cu^{2+}, Ni^{2+} Mn^{2+}, and Co^{2+} compared to Zn^{2+}, Cd^{2+}, and Mg^{2+}. The Fe^{2+} linker had the highest conductivity for all CPs. However, it was observed that low-spin Fe^{2+} complexes resulted in a much larger bandgap, only slightly better than Mg^{2+}. From DFT calculations of the band structure, closed shelled ions like Zn^{2+} and Cd^{2+} showed no contribution to the ligand bandgap. Open-shell ions participated in both the valence and conduction bands: The more electronegative ions, like Cu^{2+}, lowered the conduction band and the more electron positive ions, like high spin Fe^{2+}, raised the valence band, effectively lowering the bandgap. It is possible that utilizing transition metal ions with higher energy valence electrons such as high spin Cu^{2+} and Fe^{2+} ions will result in a lower bandgap.

Tang *et al.* systematically studied the band structure and electronic properties of M-BHT (BHT = benzenehexathiol; M = Mg, Ca, Zn, Cd, Ge, and Sn) using DFT calculations; the band gaps and the electron and hole masses were calculated and are shown in Table II.[92] The p-d coupling between the metal and S-C bands significantly delocalize the wave function of the band edge states and reduce the effective mass. As the p-d coupling increases from group IIA, IVA to IIB metals, the hole effective masses decrease significantly. As the wave characteristics of the conduction band minimum states change from the s orbitals (IIB) to hybrid pi states (IIA) and p states (IVA), their wave functions are more localized and electronic effective mass increases. $Zn_3S_6C_6$ and $Cd_3S_6C_6$ show promise as 2D semiconductors with excellent electronic and hole transport properties.

Due to the natural porosity of larger multilayer CPs, guest molecules can be introduced into their pores that can induce new electronic pathways and interactions. In one case, these guest molecules can act as bridges between secondary building units to induce through-bond transport. For example, 7,7,8,8-tetracyanoquinodimethane (TCNQ) molecules are highly conjugated and redox-active molecules that can be introduced into 2D CP frameworks as guest molecules. Nie and

TABLE II. The bandgap and hole and electron effective masses m∗ calculated by the Heyd-Scuseria-Ernzerhof hybrid functional of M-BHT.[92]

Metal	Eg (eV)	Hole m^*	Electron m^*
Mg	3.25	2.389	0.363
Ca	2.50	2.560	0.390
Zn	2.12	0.269	0.237
Cd	1.75	0.268	0.223
Ge	1.73	0.731	1.004
Sn	1.80	0.895	1.047

co-workers identified over 100 experimentally known CPs and utilized DFT calculations to provide structural information.[93] They condensed this into a recommendation of ten promising electrically conductive materials that can strongly coordinate with TCNQ through dimeric Cu paddlewheels to create 2D conducting chains. Utilizing the recommendations as a guide, Sengupta *et al.* improved the conductivity of $Cu_3(BTC)_2$ CP by the incorporation of TCNQ guest molecules, resulting in an improvement in conductivity from 10^{-8} S/cm to 0.07 S/cm.[94] DFT calculations suggest that the molecules formed new delocalized charge transport pathways by binding to two open Cu sites of the CP.

Following the design principles described above, numerous electrically conductive 2D CPs have also been designed and synthesized. Large π-conjugated organic linkers were typically used to enable high electrical conductivity. In 2015, Campbell *et al.* showed that drop cast $Cu_3(HITP)_2$ pellets could have a bulk conductivity of 0.2 S/cm^{-1}.[95] With a similar organic linker, the same group demonstrated $Cu_3(HITP)_2$ sheets with 0.002 S/cm^{-1} conductivity and with Ni as the metal center, $Ni_3(HITP)_2$ pellets achieved 2 S/cm^{-1} conductivity.[96] Melot *et al.* later revealed temperature-induced semiconducting to metallic phase transition in Co-BHT 2D CPs. The transition temperature was proven to be highly dependent on the presence of guest molecules, film thickness, and defect densities.[90] Large tunability of electrical conductivity provided by ligand/metal engineering enables their potential use as supercapacitors, field effect transistors, chemiresistors, electrocatalysts, and many more electronic applications.[97]

2. Relation to optical properties

The overall consensus in the field is that there are two main causes for light emission from these layered materials. The first is emission arising from the individual building blocks of 2D polymers, and the second resulting from the electronic band structure of the entire vdW crystal lattice.

Overall, "ligand-based photoluminescence" is the most common mechanism; the extended conjugation of ligand molecules (aromatic compounds) helps to lower the molecular energy gaps into the visible range. A secondary type of emission occurs when guest species present in the pores of the layered framework serve as the luminescence center. "Metal-centered emissions" in CPs are almost exclusively from the highly luminescent lanthanide group ions (La^{3+}, Eu^{3+}).[98] Lanthanide ions can produce emissions covering the entire UV to near infrared spectrum. The emission originates from their unique f-f electronic transitions. Due to the shielding from the closed 5s/p orbitals, they are generally unaffected by the ligand chemistry and produce sharp and characteristic emission peaks. As shown in Fig. 9, there can be interactions between the

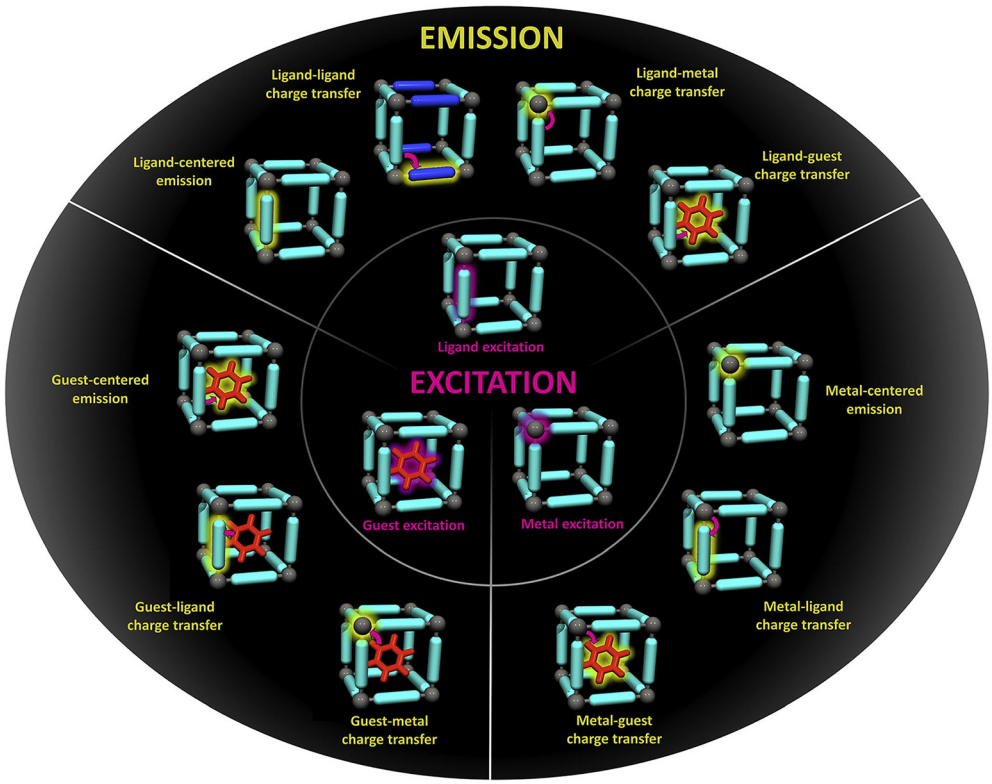

FIG. 9. Demonstration of the photoluminescence processes most commonly occurring in luminescent metal-organic frameworks and luminescent coordination polymers. The inner circle shows the excitation stage, with purple highlighting indicating the absorptive species. The outer circle shows the emission stage of photoluminescence, with yellow highlighting indicating the emissive species. Purple arrows indicate charge transfer or energy transfer processes between the absorber and emitter.[98] Reprinted with permission from W. P. Lustig and J. Li, "Luminescent metal–organic frameworks and coordination polymers as alternative phosphors for energy efficient lighting devices," Coord. Chem. Rev. **373**, 116–147 (2018). Copyright 2018 Elsevier.

guest molecule, organic ligand, and metal center that cause a multitude of charge transfers that will affect the emission.[98]

Chaudhari *et al.* synthesized optochemically responsive 2D CPs by harnessing host-guest interactions of functional sheets for the detection of organic compounds and small molecules.[99] The organic linker, 1,4-benzenedicarboxylic acid (BDC), reacted with divalent Zn^{2+} to form a white fibrous 2D CP. Figure 10(a) shows the luminescence spectra of 8 different solvent guest interactions. Four different solutions of N,N-dimethylformamide (DMF) solvent carrying zinc bis(8-hydroxyquinoline), anthracene, Al-(tris-8-hydroxyquinoline), and fluorescein demonstrate the importance of guest-host interaction in the luminescence behavior [Fig. 10(c)].

Zhang *et al.* synthesized a novel series of 2D isostructural $[CdCl(L)Eu_xTb_y(H_2O)(DMA)](NO_3)\cdot 3DMA]$ CPs where x and y are varied to create 5 novel structures.[100] Luminescence measurements indicate that the CPs exhibited characteristic sharp emission bands corresponding to the d-f transitions of the Eu(III) and Tb(III) lanthanide ions. The intensities of red and green light were modulated by tuning the molar ratios of each lanthanide component. Furthermore, it was shown that adsorption of the small molecule nitrobenzene introduced significant fluorescence quenching.

3. Relation to magnetic properties

Magnetic ordering in 2D CPs is a relatively newly discovered phenomenon and it has been shown to be possible through the anisotropic Ising model. For example, the highest Curie temperature that has been demonstrated is 50 K.[36,101,102] 2D CPs with higher temperature ferromagnetic behavior from reported theoretical studies commonly used short aromatic groups such as phthalocyanine and HAB. Generally, short organic bridges are preferred to achieve strong magnetic coupling between metal spin centers so that super-exchange interaction can be enhanced. The nitrogen functional groups are also preferred over sulfur and oxygen groups due to their more effective *p-d* exchange interactions. Manganese metal linkers are the most frequently studied because of their special electronic configuration of $3d^5 4s^2$. The use of mixed metal-organic ligands can also increase magnetic communication between metal centers.[102]

From DFT calculations, Li and co-workers predicted ferromagnetic coupling between a metal-organic cluster and organic ligand [M-octaaminophthalocyanine (OAPc) and bisphenylenediimine (Pc) linked by Ni^{2+} ions to form square planar sheets, where M = Cr, Mn, Fe, Co, Ni, Cu, and Zn].[50] They determined that the magnetic exchange energy of Mn was 183 eV, compared to negative values for the other metals. This 2D CP compound was calculated to have a Tc of 170 K for the monolayer via a Monte Carlo simulation that included the effects of magnetic anisotropy of interplanar van der Waals stacking. The strong magnetic coupling resulted from the strong hybridization between pi-symmetry orbitals of Mn and the Pc ring with the square planar Ni linkages to introduce pi electron delocalization. A possible explanation for the magnetic coupling can be from an indirect exchange interaction between the delocalized pi electrons and the

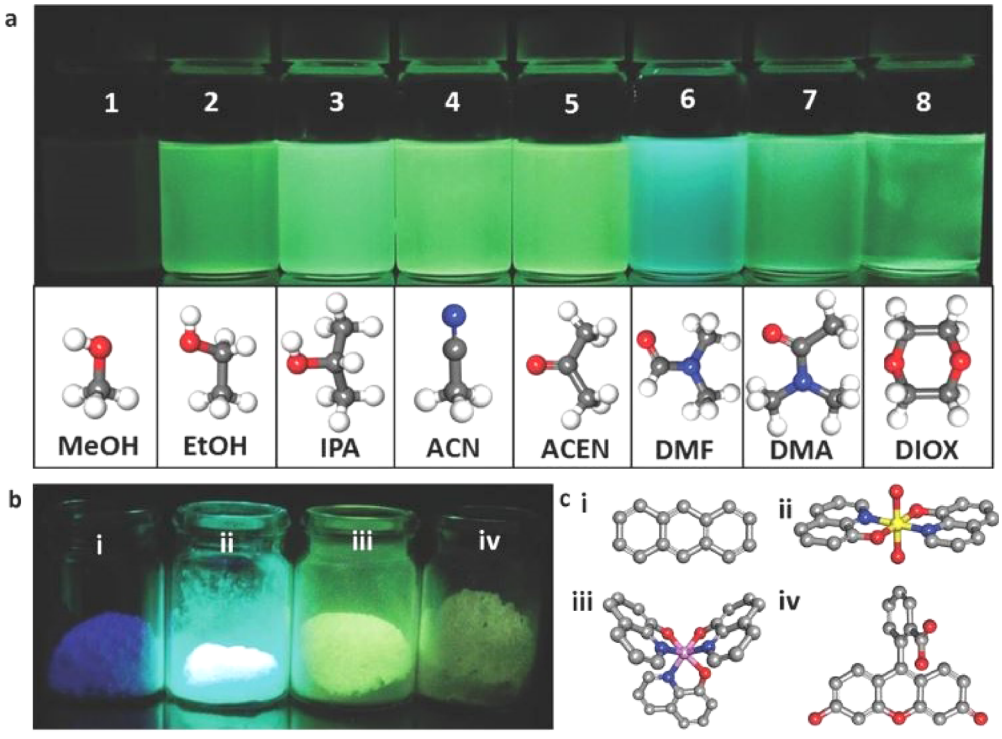

FIG. 10. Tunable optochemical behavior of zinc nanosheets. (a) Distinct modulations in emission properties of dispersions of functionalized nanosheets in a range of small-molecule solvents each comprising 5 mg of active material in a 15 ml solvent. (b) A family of host-guest materials synthesized by the one-pot supramolecular method, confining different (c) light emitting guest molecules: 1: anthracene, 2: ZnQ, 3: AlQ [Al-(tris-8-hydroxyquinoline)], and 4: fluorescein. Color scheme: zinc in yellow, aluminum in pink, nitrogen in blue, oxygen in red, carbon in gray, and hydrogen in white.[99] Reproduced with permission from Adv. Mater. **29**, 1701463 (2017). Copyright 2017 John Wiley and Sons.

localized metal center. In another study with the OAPc ligand, Zhou and Sun presented a computational comparison on monolayer sheets with transition metals from Cr, Fe, Co, Cu, Ni, Zn, and Mn.[103] Once again, only the Mn-OAPc displayed metallic d_{xz} and d_{yz} orbitals that hybridized with the p electrons of the OAPc, mediating the long-range ferromagnetic coupling with a predicted Curie temperature of 150 K. The other transition metals resulted in antiferromagnetic and non-magnetic behaviors.

Liu and Sun reported a DFT study on high temperature ferromagnetism with a Mn-HAB 2D CP.[104] The study compared the HAB ligand's magnetic behavior with that of BHT in manganese coordination polymers. The group suggested that the reduced lattice constant and improved p-d delocalization of nitrogen compared with sulfur resulted in enhanced magnetic coupling. With first principles calculations and Monte Carlo simulations based on the Ising model, the study estimated Mn-HAB's Tc at 450 K, the highest theoretically reported Curie temperature for 2D CPs. Further experimental research of OAPc and HAB ligands with manganese metal linkers is needed to realize high temperature 2D ferromagnetic coordination polymers.

4. Relation to FETs

The easy solution processability and wide tunability of electrical properties through metal ion/organic ligand engineering and the relatively low densities of CPs make them favorable for future electronic devices. The emergence of conductive 2D CPs initiated studies of field-effect transistors (FETs) with the polymeric nanosheets as active materials. Wu *et al.* first demonstrated microporous FET devices assembled with $Ni_3(HITP)_2$ as the active channel.[105] Current-voltage measurements showed excellent Ohmic contact between Au electrodes and the $Ni_3(HITP)_2$ channel. These results suggest effective modulation of carrier concentration with the gate source voltage. In addition, the transfer curve indicated p-type behavior, showing that the majority of carriers in $Ni_3(HITP)_2$ CPs are positively charged holes. The measured on/off ratio is in the range of 10^3, and the calculated hole mobility achieved was 48.6 $cm^2\ V^{-1}\ s^{-1}$, which is comparable with some of the highest recorded values for inorganic oxide semiconductors. Huang *et al.* prepared Cu-BHT thin films via a liquid-liquid interface reaction and probed the electrical behavior incorporated into FET devices. An ambipolar behavior was observed and 99 $cm^2\ V^{-1}\ s^{-1}$ electron mobility and 116 $cm^2\ V^{-1}\ s^{-1}$ hole mobility were achieved, proving balanced ambipolar charge transport properties.[44] The on-off ratio for the Cu-BHT thin films was just 10; however, this ratio could be further improved by morphology manipulation or band structure engineering of the CPs.

5. Relation to photovoltaics

Because of their Frenkel exciton behavior and small exciton binding energy, 2D CPs are regarded as potential all organic flexible photovoltaic materials. These materials could be potentially incorporated into solar cells as electron extraction layers (EELs), counter electrodes, and electron donors for organic solar cells due to their tunable electronic conductivity and behavior. Recently, work by Xing *et al.* managed to synthesize a 2D tellurophene-based coordination polymer with polyethyleneimine ethoxylate branches as an electron extraction layer (EEL) for inverted organic solar cells. The integrated EELs significantly increased the power conversion efficiency from 9.05% to 10.39%.[106] Another group, Wang *et al.*, developed stacked Zinc-porphyrin sheets as counter electrodes for dye-sensitized solar cells.[23] The power conversion efficiency was found to be 5.63%, comparable to that of platinum counter electrodes at 6.72%. Significant development is still necessary to improve the efficiency of organic solar cells and 2D CPs with their unique electronic properties and cheap costs can pave the way.

D. Heterostructure and related properties

Inheriting the vdW nature from traditional 2D materials, heterostructures of 2D polymers have been realized wherein not only one component can borrow the properties of another, but the electronic interactions between layers provide possibilities in electronic and band structure engineering. These advantages will pave new ways for material design in the application of electronic devices, sensors, and catalysis driven by electrons or photons, wherein a tunable bandgap, effective electron/mass transfer, and desired sorption kinetics are required. In general, heterostructures of 2D CPs can be achieved through direct growth onto target substrates, via the solvothermal method, or vapor deposition methods.

A report on an iron phthalocyanine (FePc)/graphene heterostructure used for electrocatalysis demonstrated this strategy clearly.[107] Single catalytic site-Fe was anchored on a 2D covalent network, which was mixed into a graphene matrix. The resulting catalyst system showed exceptional current density in oxygen reduction catalysis (four times higher than that of the benchmark Pt/C), superior power density, and cycling stability in Zn-air batteries compared with Pt/C as air electrodes. The material provided excellent catalytic activity from the iron 2D covalent organic framework material and favorable electronic conductivity due to the graphene matrix.

Additional synergistic effects at the interface can also boost the overall catalytic performance. For instance, 2D NiBDC/$Ni(OH)_2$ hybrid nanosheets were formed via the hydrothermal method wherein 2D MOF layers-NiBDC were crystallized onto prepared $Ni(OH)_2$ nanosheets.[108] After coupling, the electronic structure of Ni atoms in the $Ni(OH)_2$ component is significantly modified, leading to the generation of Ni cations with higher oxidation states, which are desirable for the oxygen reduction. The as-prepared NiBDC/$Ni(OH)_2$ heterostructures exhibited high activity, favorable kinetics, and strong durability during the catalysis. In another example, a 2D Co-CP/graphene oxide (GO) heterostructure was synthesized via solvothermal synthesis of exfoliated graphene oxide flakes in a cobalt organic solution. The hybrid membrane displayed superior sorption efficiency of toxic Cs^+ ions. It was suggested that the synergistic effects were due to the electrostatic interaction from intrinsically negative GO and positive Co-CP.

Although still in its early stages, 2D heterostructures grown on 2D vDW substrates can lead to interesting interacting properties. Recently, Kumar and co-workers were able to successfully grow 2D Co CPs directly on a graphene substrate via molecular beam epitaxy.[46] With DFT calculations and STM measurements, the group were able to study the decoupled band structure of the 2D CP. The possibility of incorporating heavier transition metals, which possess higher spin–orbit coupling, could lead to exotic quantum properties.

V. MATERIAL STABILITY

It is well known that coordination polymer structures, in general, are mechanically, thermally, and chemically less stable than their covalent polymeric counterparts.[13,14] The coordination bonds are

weaker, making them more susceptible to decomposition in aqueous and organic solutions and heat. The stability of 2D CPs can be improved by multiple factors including the choice of metal ions, organic ligands, operating environment, coordination geometry, and hydrophobicity.[109]

Coordination bonds require robust and thermodynamically stable bonds. Referencing to the Hard Acid Soft Base (HASB) theory can help design more thermodynamically stable coordination bonds. The HASB theory states that hard acids form stronger ionic bonds with hard bases while soft acids will form stronger covalent bonds with soft bases. Soft/borderline acids are transition metals with lower oxidation states and larger ionic radii such as Zn^{2+}, Pt^{2+}, Pd^{2+}, Cu^{2+}, Ni^{2+}, Mn^{2+}, Co^{2+}, Cd^{2+}, and Fe^{2+} ions. In theory, these softer acids will form stable bonds with soft/borderline bases such as the soft azolates, aromatic/phenyl ligands, thiolates, amines, and cyanates.[19,24,32,110,111] However, there also have been cases of the softer acids linking with carboxylate ligands.[70,73,112,113] Hard acids are high valent metal ions including Ti^{4+}, Zr^{4+}, Al^{3+}, Fe^{3+}, Cr^{3+}, and Ln^{3+} ions. These hard metal ions should form strong bonds with the stronger bases, primarily carboxylate-based ligands.[80,114]

Water stability is an important aspect of 2D CPs, specifically for their use in water separation and bioorganic applications. The effect of the moisture in air has also been problematic in synthesizing stable 2D CPs under ambient conditions. The air and water stability can be improved by incorporating hydrophobic functional groups into the 2D CP to obstruct the water from intrusion into the structure and attacking the metal center.[116] The metal linker should be connected to functional groups surrounded by phenyl or methyl-based ligands to provide steric and hydrophobic hindrance to water molecules.[69,74,84,115,117,118] An example is shown in Figs. 11(a) and 11(b).[74,115]

VI. PERSPECTIVES

A. Fundamental insights into defect engineering

Defects have been known to pose a great influence on electrical, optical, magnetic, chemical, and mechanical properties of materials. Despite some efforts reported in defect engineering in 3D CPs, a more comprehensive study is required for understanding the formation mechanism and types of defects in 2D CPs. This is mainly due to a limitation in the characterization tools, which are not usually geared toward handling atomically thin, delicate organic materials for defect characterization. Standard defect characterization techniques used for inorganic materials, including HRTEM, SIMS, and STM, often fail to access such information.

Regardless, the researchers independently working on 2D CP synthesis and material characterization must forge new interdisciplinary collaborations to interconnect 2D CP synthesis, atomic structure, and performance. These efforts will create new structure-property-performance relationships that could revolutionize the field of 2D CPs. To exploit the properties brought about by various defects, fast, accurate, and cost-effective defect characterization methods are needed. Synthesis methods must involve *in situ* and *ex situ* processes to control the types and concentration of defects. In particular, 0D point defects and 1D grain boundaries are likely to play a crucial role in dictating the overall properties of 2D CPs. First, the effects of these imperfections on the optical and electronic properties must be well understood and those promising ones must be introduced on demand with spatio-temporal control.[119]

1. Manufacturing challenges

From the manufacturing perspective, we foresee that more controlled growth processes are crucial to eliminate or limit the number of defects for the application of these material systems. More studies will be needed to answer the question of the typical density of imperfections in existing 2D CPs. This first requires a fundamental understanding of the growth thermodynamics and kinetics, which can then be harnessed to produce materials with ultimate crystalline perfection.

Another manufacturing challenge will be thickness control. Current state of the art methods have enabled researchers to achieve large scale 2D CP materials. But in these larger material systems, rarely was the thickness controlled. Considering how 2D layered materials

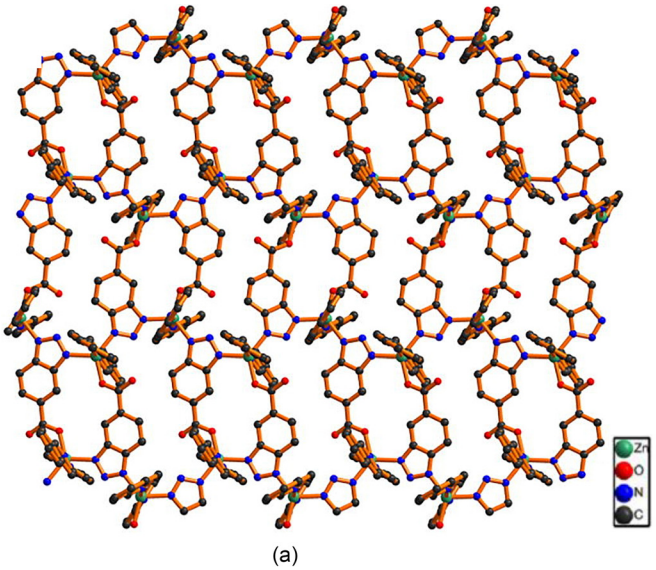

(a)

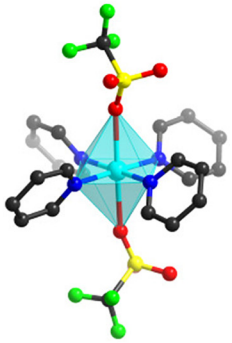
(b)

FIG. 11. (a) Schematic representation of the 2D network by Ning *et al.*[115] Reprinted with permission Ning *et al.*, "A 2D water-stable metal–organic framework for fluorescent detection of nitroaromatics," Polyhedron **155**, 457–463 (2018). Copyright 2018 Elsevier. (b) Schematic representation of unit cell by Xu *et al.* The C, O, S, F, and Cu atoms are gray, red, yellow, green, and teal, respectively. Reprinted and adapted with permission from Xu *et al.*, J. Am. Chem. Soc. **139**, 8312 (2017). Copyright 2017 American Chemical Society.

behave differently compared with their bulk counterparts, it is essential to achieve control over the thickness in the manufacturing process. While this is a relatively easy task for inorganic 2D materials through well-controlled chemical vapor deposition or molecular beam epitaxy techniques, etc., polymeric materials require solution processing in which far fewer techniques are available to produce monolayer films on a large scale. It is also expected that completely new growth techniques will emerge to deposit these 2D CP materials, especially as synthesis and material characterization efforts begin to coalesce. One potential exciting route is the *in situ* MBE process wherein organic flux is injected at selected rates under ultrahigh vacuum conditions to enable self-assembly of coordination structures on the surface.

2. Informed ligand and linker engineering

While theoretical calculations have overviewed the general trends, such as those of band gaps and conductivities of these materials, experimental investigations are mostly limited to electrical properties of the material. It will be important to see how the electronic bandgap, optical bandgap, exciton binding energy, thermal conductivity, and fundamental optical behavior (reflection, transmission, absorption) change through metal and organic linker designs. There are many fundamental questions that are awaiting to be answered: How does the metal linker influence the electronic and optical bandgap of the material? How does the ligand overall influence the optical properties of these systems? What is the exciton binding energy? How do these properties change for different thickness values? More comprehensive and computational studies are needed to provide further insights into their optical and excitonic properties. Only after completion of these studies can we further understand the future applications related to these material systems.

B. Future horizons

As mentioned earlier, the fundamental properties of these 2D polymeric materials are not well known; thus, the field of optics and electronics is still at its seminal stages. With that in mind, there are a number of attributes related to the crystallinity or type of metal linkers involved in the crystal structure that provides general hints about the potential application areas without necessarily knowing these fundamental properties. Considering their unique chemical structure and availability of single atom (catalysts), heterogeneous catalysis and gas separation applications come to mind immediately.

By appropriately designing the CP composition, they could be incorporated into photovoltaic devices, light emission devices, and such applications. In the past, organic electronics such as solar cells have gained massive attention. These materials have shown attractive bandgap values but their effective masses and conductivity values must be further engineered. The near limitless combinations of ligands and metals in constructing 2D coordination polymers allow for such specific tailoring of band gaps and charge mobilities. There are challenges awaiting such as electrical conductivity, which is highly dependent on the intrinsic defect density of material systems. At present, this field is rather speculative based on the lack of experimental evidence, but a promising application nonetheless. More experimental research and computational studies such as Tang *et al.* is required to elevate these material systems into the organic electronic field.[92] Finally, an integrated effort to optimize the synthesis of a material with promising performance and engineer the material to be processable in large surface area formats is critical for the field to impact society. Without this effort, only new and interesting fundamental physics and chemistries will be discovered.

C. Other aggressive research directions

1. Moire patterns and superlattices

We foresee more aggressive research will takeoff in the upcoming months, years, and perhaps decades. Recent theoretical and experimental studies have shown that stacking two similar 2D materials with a small twist angle opens up entirely new classes of materials called twistronic materials or in generally twistronics. Studies on 2D systems have already shown that Moire superlattices created by twisting adjacent layers with respect to each other gives rise to unusual quantum properties including superconductivity, Moire excitons, Mott-like insulators, etc.[120–123] Similar manipulation of interlayer interaction could be achieved in 2D CPs, with longer periodicity and potentially more exotic properties. Many questions in this niche field could potentially serve as guide in 2D CP twistronics or Moire superlattices. For example, how do the optical properties change when two different CPs stack onto each other with a particular angle? Can one engineer the effective pore size by twisting these layers? Can metal link atom interaction be enhanced at magical twist angles to engineer magnetism? Answers to these questions are likely to open new directions and subfields.

2. Magnetism

While magnetic order in two-dimensions and especially in organic materials might sound counterintuitive, more thought must be put in to determine the potential of 2D CPs in 2D magnetism field. As discussed earlier, theoretical studies already suggest potentially exotic magnetic order in 2D CPs with selected types of ligand chemistries. The question becomes how can one synthesize these materials that could exhibit ferromagnetic or ferrimagnetic order in 2D? If magnetic ordering is possible, theoretical and experimental studies must develop theories that could potentially deviate from Heisenberg and Ising models in 2D. Another question is related to their Curie temperature when the material undergoes paramagnetic to ferromagnetic crossover at lower temperatures. Is it possible to design materials that exhibit high T_c values for potential application? What are the design considerations in engineering the T_c values? Finally, using heavy metal atoms from Actinide or pnictine families might create completely new correlated systems in quantum fields. One particular example could be the realization of Kondo lattices using 2D polymers.

3. Quantum applications

Quantum technologies are expected to be the future of information processing and computation. High density and efficient single photon emitters are necessary for the future of quantum computing. Molecular emitters have been suggested as potential candidates for single emitter quantum systems due to their sharp emissions and tunable range of photon energies.

Paramagnetic coordination complexes have been proposed as alternative molecular spin qubits with molecular electronic spin orientation and superposition as encoded quantum bit states.[124] Urtizberea

et al. designed 2D [CuTCPP]Zn_2 framework (TCPP: tetrakis(4-carboxyphenyl)-porphyrin).[60] In this system, paramagnetic CuTCPP behaves as a molecule qubit with its singular electron spin and Zn as its diamagnetic nodes. The concentration of the qubit within the nanosheets was controlled through dilution of the solution with the metal free porphyrin ligands. Pulse electron paramagnetic resonance spectroscopy showed phase memory times of 1.04 μs at 6 K and 0.39 μs at 90 K. Their work demonstrated the potential of 2D coordination complexes as molecular qubits, although longer coherence times and precise atomic control of magnetic dilution need to be further explored.

Topological insulators (TIs), also known as quantum spin Hall insulators, are a class of quantum materials that possess symmetry-protected conductive surface states, which are promising candidates for spintronic devices and quantum computing applications. Since the experimental verification of the TI nature of bismuth antimonide, generations of inorganic TI materials have been predicted and synthesized.[125] In 2013, Wang *et al.* first designed a hexagonal triphenyl-lead ($Pb(C_6H_5)_3$) lattice, which showed a robust, nontrivial, gapless edge in DFT calculations.[126] The same group later identified topological states in an experimentally realized 2D $Ni_3C_{12}S_{12}$ Kagome lattice. This structure contained a π conjugated nickel-bis-dithiolene network and theoretical calculations showed topological states in both the Dirac band and a flatband.[127] Another experimentally synthesized 2D CP, Cu–dicyanoanthracene (DCA), was theoretically predicted to have a Dirac point at the Fermi level and semi-infinite Dirac edge states within spin–orbit coupling gaps.[128] Zhang *et al.* attributed its topological properties to a proper number of electrons in hybridized bands from Cu ions and DCA molecules. Extended studies predicted Au and cyanogen networks with a similar structure are also potential TIs. In 2018, Hsu *et al.* systematically explored metal dicyanobenzenes with elements ranging from IIIA, IVA, VA, VIA, IB, and Pt. Multiple TIs were identified from these materials. Interestingly, p-type Bi-DCA exhibited nearly flat Chern bands from calculations, suggesting a quantum anomalous Hall (QAH) phase.[129] Spontaneous magnetization combined with spin–orbit coupling can potentially give rise to quantized Hall conductivity. Several teams used DFT and tight-binding approximation to search for 2D CPs that showed a QAH effect. From their research, Mn-DCAs, triphenyl-Mn and indium-phenylene were identified to be potential candidates.[130,131]

Though most of the work toward finding potential TIs in 2D CPs is limited to theoretical calculations, advances in synthesis and manufacturing of 2D CPs would allow integration of the mechanical flexibility and tunability into fundamental physics exploration and quantum device applications.

VII. CONCLUSIONS

The future for 2D CPs is extremely bright. The potential applications for this unique class of materials are nearly limitless, in part due to the endless combinations of building blocks that can be combined to produce tailor-made materials. The seminal work in this field has produced preliminary design rules that help us understand which ligands and metals can be combined, and in what fashion, to control the thermal, mechanical, magnetic, and optoelectronic properties. However, the community has arrived at the crossroads where the synthesis and characterization must integrate in order to accelerate material discovery, yield new and fundamental structure-property-performance relationships, and enable scalable manufacturing processes. This will require new instrumentation and inform limitations and needs in characterization. This overview, we hope, will serve as a roadmap and framework for identifying new and exciting material targets, strategies for engineering desirable properties, and conduits to streamline the manufacturing and processing of these exciting materials.

ACKNOWLEDGMENTS

S.T. acknowledges support from Nos. NSF DMR-1552220, NSF DMR 1838443, and CMMI-1561839, and Army Research Office Materials Program (PM: Pani Varanasi). M.D.G. acknowledges support from No. NSF CBET-1836719, the Army Research Office (No. W911NF-18-1-0412), and NASA (No. 80NSSC18K1508).

REFERENCES

[1]M. Zeng, Y. Xiao, J. Liu, K. Yang, and L. Fu, Chem. Rev. **118**, 6236 (2018).
[2]S. Manzeli, D. Ovchinnikov, D. Pasquier, O. V. Yazyev, and A. Kis, Nat. Rev. Mater. **2**, 17033 (2017).
[3]K. Zhang, Y. Feng, F. Wang, Z. Yang, and J. Wang, J. Mater. Chem. C **5**, 11992 (2017).
[4]M. Khazaei, A. Mishra, N. S. Venkataramanan, A. K. Singh, and S. Yunoki, Curr. Opin. Solid State Mater. Sci. **23**, 164 (2019).
[5]H. An, T. Habib, S. Shah, H. Gao, M. Radovic, M. J. Green, and J. L. Lutkenhaus, Sci. Adv. **4**, eaaq0118 (2018).
[6]P. Lakhe, E. M. Prehn, T. Habib, J. L. Lutkenhaus, M. Radovic, M. S. Mannan, and M. J. Green, Ind. Eng. Chem. Res. **58**, 1570 (2019).
[7]H. An, T. Habib, S. Shah, H. Gao, A. Patel, I. Echols, X. Zhao, M. Radovic, M. J. Green, and J. L. Lutkenhaus, ACS Appl. Nano Mater. **2**, 948 (2019).
[8]T. Habib, X. Zhao, S. A. Shah, Y. Chen, W. Sun, H. An, J. L. Lutkenhaus, M. Radovic, and M. J. Green, npj 2D Mater. Appl. **3**, 8 (2019).
[9]Y. Chen, Y. Sun, J. Peng, J. Tang, K. Zheng, and Z. Liang, Adv. Mater. **30**, 1703487 (2018).
[10]C. E. Boott, A. Nazemi, and I. Manners, Angew. Chem., Int. Ed. **54**, 13876 (2015).
[11]C. H. Hendon, A. J. Rieth, M. D. Korzyński, and M. Dincă, ACS Cent. Sci. **3**, 554 (2017).
[12]S. L. Cai, W. G. Zhang, R. N. Zuckermann, Z. T. Li, X. Zhao, and Y. Liu, Adv. Mater. **27**, 5762 (2015).
[13]J. W. Colson and W. R. Dichtel, Nat. Chem. **5**, 453 (2013).
[14]D. Rodríguez-San-Miguel, P. Amo-Ochoa, and F. Zamora, Chem. Commun. **52**, 4113 (2016).
[15]M. Zhao, Q. Lu, Q. Ma, and H. Zhang, Small Methods **1**, 1600030 (2017).
[16]M. Zhao, Y. Huang, Y. Peng, Z. Huang, Q. Ma, and H. Zhang, Chem. Soc. Rev. **47**, 6267 (2018).
[17]L. Cao, T. Wang, and C. Wang, Chin. J. Chem. **36**, 754 (2018).
[18]I.-F. Chen, C.-F. Lu, and W.-F. Su, Langmuir **34**, 15754 (2018).
[19]R. Makiura and O. Konovalov, Dalton Trans. **42**, 15931 (2013).
[20]Y. Jiang, G. Hee Ryu, S. Hun Joo, X. Chen, S. Hwa Lee, X. Chen, M. Huang, X. Wu, D. Luo, Y. Huang, J. Hyeon Lee, B. Wang, X. Zhang, S. Kyu Kwak, Z. Lee, and R. S. Ruoff, ACS Appl. Mater. Interfaces **9**, 28107 (2017).
[21]R. Makiura, K. Tsuchiyama, and O. Sakata, CrystEngComm **13**, 5538 (2011).
[22]Z.-G. Gu and J. Zhang, Coord. Chem. Rev. **378**, 513 (2019).
[23]Y. Y. Wang, S. M. Chen, R. Haldar, C. Wöll, Z. G. Gu, and J. Zhang, Adv. Mater. Interfaces **5**, 1800985 (2018).
[24]S. Hu, J. Yan, X. Huang, L. Guo, Z. Lin, F. Luo, B. Qiu, K. Y. Wong, and G. Chen, Sens. Actuators, B **267**, 312 (2018).
[25]A. W. Kelly, A. M. Wheaton, A. D. Nicholas, H. H. Patterson, and R. D. Pike, J. Inorg. Organomet. Polym. Mater. **28**, 528 (2018).
[26]B. Wurster, D. Grumelli, D. Hö, R. Gutzler, and K. Kern, J. Am. Chem. Soc. **138**, 3623 (2016).
[27]E. Ahvenniemi and M. Karppinen, Chem. Commun. **52**, 1139 (2016).

[28]L. D. Salmi, M. J. Heikkilä, E. Puukilainen, T. Sajavaara, D. Grosso, and M. Ritala, Microporous Mesoporous Mater. **182**, 147 (2013).
[29]Y. Zhao, N. Kornienko, Z. Liu, C. Zhu, S. Asahina, T.-R. Kuo, W. Bao, C. Xie, A. Hexemer, O. Terasaki, P. Yang, and O. M. Yaghi, J. Am. Chem. Soc. **137**, 2199 (2015).
[30]T. Wen, D. X. Zhang, and J. Zhang, Inorg. Chem. **52**, 12 (2013).
[31]Z. Hu, E. M. Mahdi, Y. Peng, Y. Qian, B. Zhang, N. Yan, D. Yuan, J. C. Tan, and D. Zhao, J. Mater. Chem. A **5**, 8954 (2017).
[32]Y. H. Zhou and Z. Y. Wang, Bull. Korean Chem. Soc. **36**, 618 (2015).
[33]R. Yan, Y. Zhao, H. Yang, X. J. Kang, C. Wang, L. L. Wen, and Z. Da Lu, Adv. Funct. Mater. **28**, 1802021 (2018).
[34]S. C. Junggeburth, L. Diehl, S. Werner, V. Duppel, W. Sigle, and B. V. Lotsch, J. Am. Chem. Soc. **135**, 6157 (2013).
[35]M. Zhao, Y. Wang, Q. Ma, Y. Huang, X. Zhang, J. Ping, Z. Zhang, Q. Lu, Y. Yu, H. Xu, Y. Zhao, and H. Zhang, Adv. Mater. **27**, 7372 (2015).
[36]S. Zhou, W. Shi, M. Wang, Y. Sun, Z. Zhang, E. Zschech, C. Felser, P. Adler, X. Feng, D. C. Tranca, R. Dong, F. Liu, Z. Liao, Z. Zhang, and S. C. B. Mannsfeld, Nat. Commun. **9**, 2637 (2018).
[37]L. Cao, Z. Lin, F. Peng, W. Wang, R. Huang, C. Wang, J. Yan, J. Liang, Z. Zhang, T. Zhang, L. Long, J. Sun, and W. Lin, Angew. Chem., Int. Ed. **55**, 4962 (2016).
[38]P. Amo-Ochoa, L. Welte, R. González-Prieto, P. J. Sanz Miguel, C. J. Gómez-García, E. Mateo-Martí, S. Delgado, J. Gómez-Herrero, and F. Zamora, Chem. Commun. **46**, 3262 (2010).
[39]M. J. Cliffe, E. Castillo-Martínez, Y. Wu, J. Lee, A. C. Forse, F. C. N. Firth, P. Z. Moghadam, D. Fairen-Jimenez, M. W. Gaultois, J. A. Hill, O. V. Magdysyuk, B. Slater, A. L. Goodwin, and C. P. Grey, J. Am. Chem. Soc. **139**, 5397 (2017).
[40]A. Gallego, C. Hermosa, O. Castillo, I. Berlanga, C. J. Gómez-García, E. Mateo-Martí, J. I. Martínez, F. Flores, C. Gómez-Navarro, J. Gómez-Herrero, S. Delgado, and F. Zamora, Adv. Mater. **25**, 2141 (2013).
[41]A. Kondo, C. C. Tiew, F. Moriguchi, and K. Maeda, Dalton Trans. **42**, 15267 (2013).
[42]*Design and Construction of Coordination Polymers*, edited by M.-C. Hong and L. Chen (John Wiley & Sons, Inc., Hoboken, NJ, USA, 2009).
[43]A. Mukhopadhyay, V. K. Maka, G. Savitha, and J. N. Moorthy, Chem **4**, 1059 (2018).
[44]X. Huang, P. Sheng, Z. Tu, F. Zhang, J. Wang, H. Geng, Y. Zou, C. Di, Y. Yi, Y. Sun, W. Xu, and D. Zhu, Nat. Commun. **6**, 7408 (2015).
[45]N. Lahiri, N. Lotfizadeh, R. Tsuchikawa, V. V. Deshpande, and J. Louie, J. Am. Chem. Soc. **139**, 19 (2017).
[46]A. Kumar, K. Banerjee, A. S. Foster, and P. Liljeroth, Nano Lett. **18**, 5596 (2018).
[47]M. Haruta and H. Kurata, Sci. Rep. **2**, 252 (2012).
[48]L. P. Zhang, H. W. Hou, Y. T. Fan, and F. H. Cheng, Chin. J. Inorg. Chem. **16**, 10 (2000).
[49]V. Chernikova, O. Shekhah, I. Spanopoulos, P. N. Trikalitis, and M. Eddaoudi, Chem. Commun. **53**, 6191 (2017).
[50]W. Li, L. Sun, J. Qi, P. Jarillo-Herrero, M. Dincă, and J. Li, Chem. Sci. **8**, 2859 (2017).
[51]S. Chen, J. Dai, and X. C. Zeng, Phys. Chem. Chem. Phys. **17**, 5954 (2015).
[52]Z. Shi and N. Lin, J. Am. Chem. Soc. **131**, 5376 (2009).
[53]E. L. Spitler, J. W. Colson, F. J. Uribe-Romo, A. R. Woll, M. R. Giovino, A. Saldivar, and W. R. Dichtel, Angew. Chem., Int. Ed. **51**, 2623 (2012).
[54]L. H. Li, J. Q. Li, and L. M. Wu, J. Phys. Chem. C **116**, 9235 (2012).
[55]M. Abel, S. Clair, O. Ourdjini, M. Mossoyan, and L. Porte, J. Am. Chem. Soc. **133**, 1203 (2011).
[56]H. Nagatomi, N. Yanai, T. Yamada, K. Shiraishi, and N. Kimizuka, Chemistry **24**, 1806 (2018).
[57]H. Zhong, K. H. Ly, M. Wang, Y. Krupskaya, X. Han, J. Zhang, J. Zhang, V. Kataev, B. Büchner, I. M. Weidinger, S. Kaskel, P. Liu, M. Chen, R. Dong, and X. Feng, Angew. Chem., Int. Ed. **58**, 10677 (2019).
[58]G. R. Monama, K. D. Modibane, K. E. Ramohlola, K. M. Molapo, M. J. Hato, M. D. Makhafola, G. Mashao, S. B. Mdluli, and E. I. Iwuoha, Int. J. Hydrogen Energy **15**, 102564 (2019).
[59]H. Jia, Y. Yao, J. Zhao, Y. Gao, Z. Luo, and P. Du, J. Mater. Chem. A **6**, 1188 (2018).
[60]A. Urtizberea, E. Natividad, P. J. Alonso, M. A. Andrés, I. Gascón, M. Goldmann, and O. Roubeau, Adv. Funct. Mater. **28**, 1801695 (2018).
[61]S. Motoyama, R. Makiura, O. Sakata, and H. Kitagawa, J. Am. Chem. Soc. **133**, 5640 (2011).
[62]B. Zhu, X. Zhang, B. Zeng, M. Li, and M. Long, Org. Electron. **49**, 45 (2017).
[63]Y. Li, Z. Gao, F. Chen, C. You, H. Wu, K. Sun, P. An, K. Cheng, C. Sun, X. Zhu, and B. Sun, ACS Appl. Mater. Interfaces **10**, 30930 (2018).
[64]Y. Zhao, L. Jiang, L. Shangguan, L. Mi, A. Liu, and S. Liu, J. Mater. Chem. A **6**, 2828 (2018).
[65]G. Gao, E. R. Waclawik, and A. Du, J. Catal. **352**, 579 (2017).
[66]J. Park, A. C. Hinckley, Z. Huang, D. Feng, A. A. Yakovenko, M. Lee, S. Chen, X. Zou, and Z. Bao, J. Am. Chem. Soc. **140**, 14533 (2018).
[67]X. Zhang, P. Zhang, C. Chen, J. Zhang, G. Yang, L. Zheng, J. Zhang, and B. Han, Green Chem. **21**, 54 (2019).
[68]L.-X. You, B.-B. Zhao, H.-J. Liu, S.-J. Wang, G. Xiong, Y.-K. He, F. Ding, J. J. Joos, P. F. Smet, and Y.-G. Sun, CrystEngComm **20**, 615 (2018).
[69]X. Guo, P. Wang, J. Xu, L. Shen, J. Sun, Y. Tao, X. Chen, S. Jing, L. Wang, and Y. Fan, Inorg. Chim. Acta **479**, 213 (2018).
[70]R. Dai, X. Zhang, M. Liu, Z. Wu, and Z. Wang, J. Membr. Sci. **573**, 46 (2019).
[71]S. R. Batten, S. M. Neville, and D. R. Turner, *Coordination Polymers* (Royal Society of Chemistry, Cambridge, 2008).
[72]R. Sakamoto, K. Takada, T. Pal, H. Maeda, T. Kambe, and H. Nishihara, Chem. Commun. **53**, 5781 (2017).
[73]Y. H. Luo, C. Chen, C. He, Y. Y. Zhu, D. L. Hong, X. T. He, P. J. An, H. S. Wu, and B. W. Sun, ACS Appl. Mater. Interfaces **10**, 28860 (2018).
[74]M. Xu, S. Yuan, X.-Y. Chen, Y.-J. Chang, G. Day, Z.-Y. Gu, and H.-C. Zhou, J. Am. Chem. Soc. **139**, 8312 (2017).
[75]H. Hijikata and Y. Hijikata, Inorg. Chem. **52**, 3634 (2013).
[76]Q. Yan, Y. Lin, P. Wu, L. Zhao, L. Cao, L. Peng, C. Kong, and L. Chen, ChemPlusChem **78**, 86 (2013).
[77]M. Xu, S. S. Yang, and Z. Y. Gu, Chemistry **24**, 15131 (2018).
[78]A. Zirehpour, A. Rahimpour, and M. Ulbricht, J. Membr. Sci. **531**, 59 (2017).
[79]A. Morsali and L. Hashemi, *Main Group Metal Coordination Polymers* (John Wiley & Sons, Inc., Hoboken, NJ, USA, 2017).
[80]Y. H. Li, S. L. Wang, Y. C. Su, B. T. Ko, C. Y. Tsai, and C. H. Lin, Dalton Trans. **47**, 9474 (2018).
[81]G. Zhan and H. C. Zeng, Adv. Funct. Mater. **26**, 3268 (2016).
[82]F.-X. Wang, X.-H. Yi, C.-C. Wang, and J.-G. Deng, Chin. J. Catal. **38**, 2141 (2017).
[83]D. Sadhukhan, A. Ray, R. J. Butcher, C. J. Gómez García, B. Dede, and S. Mitra, Inorg. Chim. Acta **376**, 245 (2011).
[84]J. Chen, Y. Shu, H. Li, Q. Xu, and X. Hu, Talanta **189**, 254 (2018).
[85]A. Dhakshinamoorthy, Z. Li, and H. Garcia, Chem. Soc. Rev. **47**, 8134 (2018).
[86]T. He, B. Ni, S. Zhang, Y. Gong, H. Wang, L. Gu, J. Zhuang, W. Hu, and X. Wang, Small **14**, 1703929 (2018).
[87]C. G. Silva, A. Corma, and H. García, J. Mater. Chem. **20**, 3141 (2010).
[88]M. Usman, S. Mendiratta, and K. L. Lu, Adv. Mater. **29**, 1605071 (2017).
[89]D. Tiana, C. H. Hendon, A. Walsh, and T. P. Vaid, Phys. Chem. Chem. Phys. **16**, 14463 (2014).
[90]A. J. Clough, J. M. Skelton, C. A. Downes, A. A. de la Rosa, J. W. Yoo, A. Walsh, B. C. Melot, and S. C. Marinescu, J. Am. Chem. Soc. **139**, 10863 (2017).
[91]L. Sun, C. H. Hendon, S. S. Park, Y. Tulchinsky, R. Wan, F. Wang, A. Walsh, and M. Dincă, Chem. Sci. **8**, 4450 (2017).
[92]L. P. Tang, L. M. Tang, H. Geng, Y. P. Yi, Z. Wei, K. Q. Chen, and H. X. Deng, Appl. Phys. Lett. **112**, 012101 (2018).
[93]X. Nie, A. Kulkarni, and D. S. Sholl, J. Phys. Chem. Lett. **6**, 1586 (2015).
[94]A. Sengupta, S. Datta, C. Su, T. S. Herng, J. Ding, J. J. Vittal, and K. P. Loh, ACS Appl. Mater. Interfaces **8**, 16154 (2016).
[95]D. Sheberla, S. F. Liu, T. M. Swager, M. Dincă, and M. G. Campbell, Angew. Chem., Int. Ed. **54**, 4349 (2015).
[96]M. G. Campbell, S. F. Liu, T. M. Swager, and M. Dincă, J. Am. Chem. Soc. **137**, 13780 (2015).
[97]M. Ko, L. Mendecki, and K. A. Mirica, Chem. Commun. **54**, 7873 (2018).
[98]W. P. Lustig and J. Li, Coord. Chem. Rev. **373**, 116 (2018).
[99]A. K. Chaudhari, H. J. Kim, I. Han, and J. C. Tan, Adv. Mater. **29**, 1701463 (2017).

[100]S.-R. Zhang, D.-Y. Du, J.-S. Qin, S.-L. Li, W.-W. He, Y.-Q. Lan, and Z.-M. Su, Inorg. Chem. **53**, 8105 (2014).
[101]D. G. Branzea, L. Sorace, C. Maxim, M. Andruh, and A. Caneschi, Cryst. Growth Des. **47**, 6590 (1990).
[102]G. Mínguez Espallargas and E. Coronado, Chem. Soc. Rev. **47**, 533 (2018).
[103]J. Zhou and Q. Sun, J. Am. Chem. Soc. **133**, 15113 (2011).
[104]J. Liu and Q. Sun, ChemPhysChem **16**, 614 (2015).
[105]G. Wu, J. Huang, Y. Zang, J. He, and G. Xu, J. Am. Chem. Soc. **139**, 1360 (2017).
[106]H. Huang, X. Wu, J. Lu, Y. Chen, T. Zhu, A. Peng, W. Xing, and P. Ye, J. Power Sources **401**, 13 (2018).
[107]P. Peng, L. Shi, F. Huo, C. Mi, X. Wu, S. Zhang, and Z. Xiang, Sci. Adv. **5**, eaaw2322 (2019).
[108]D. Zhu, J. Liu, L. Wang, Y. Du, Y. Zheng, K. Davey, and S.-Z. Qiao, Nanoscale **11**, 3599 (2019).
[109]S. Yuan, L. Feng, K. Wang, J. Pang, M. Bosch, C. Lollar, Y. Sun, J. Qin, X. Yang, P. Zhang, Q. Wang, L. Zou, Y. Zhang, L. Zhang, Y. Fang, J. Li, and H. C. Zhou, Adv. Mater. **30**, 17044303 (2018).
[110]J. Park, M. Lee, D. Feng, Z. Huang, A. C. Hinckley, A. Yakovenko, X. Zou, Y. Cui, and Z. Bao, J. Am. Chem. Soc. **140**, 10315 (2018).
[111]F. Li, X. Zhang, X. Liu, and M. Zhao, ACS Appl. Mater. Interfaces **10**, 15012 (2018).
[112]Y. Z. Tang, X. Sen Wang, T. Zhou, and R. G. Xiong, Cryst. Growth Des. **6**, 11 (2006).
[113]H. Lu and S. Zhu, Eur. J. Inorg. Chem. **2013**, 1294.
[114]S. Sharif, O. Şahin, B. Khan, and I. U. Khan, J. Coord. Chem. **68**, 2725 (2015).
[115]S. Ning, H. Chen, S. Zhang, and P. Cheng, Polyhedron **155**, 457 (2018).
[116]N. C. Burtch, H. Jasuja, and K. S. Walton, Chem. Rev. **114**, 10575 (2014).
[117]Y. Zhang and J. Wang, Inorg. Chim. Acta **477**, 8 (2018).
[118]Y. Liu, Y. Han, Z. Zhang, W. Zhang, W. Lai, Y. Wang, and R. Cao, Chem. Sci. **10**, 2613 (2019).
[119]G. Ye, Y. Gong, J. Lin, B. Li, Y. He, S. T. Pantelides, W. Zhou, R. Vajtai, and P. M. Ajayan, Nano Lett. **16**, 1097 (2016).
[120]C. Jin, E. C. Regan, A. Yan, M. I. B. Utama, D. Wang, S. Zhao, Y. Qin, S. Yang, Z. Zheng, S. Shi, K. Watanabe, T. Taniguchi, S. Tongay, A. Zettl, and F. Wang, Nature **567**, 76 (2019).
[121]K. Tran, G. Moody, F. Wu, X. Lu, J. Choi, K. Kim, A. Rai, D. A. Sanchez, J. Quan, A. Singh, J. Embley, A. Zepeda, M. Campbell, T. Autry, T. Taniguchi, K. Watanabe, N. Lu, S. K. Banerjee, K. L. Silverman, S. Kim, E. Tutuc, L. Yang, A. H. MacDonald, and X. Li, Nature **567**, 71 (2019).
[122]Y. Cao, V. Fatemi, A. Demir, S. Fang, S. L. Tomarken, J. Y. Luo, J. D. Sanchez-Yamagishi, K. Watanabe, T. Taniguchi, E. Kaxiras, R. C. Ashoori, and P. Jarillo-Herrero, Nature **556**, 80 (2018).
[123]Y. Cao, V. Fatemi, S. Fang, K. Watanabe, T. Taniguchi, E. Kaxiras, and P. Jarillo-Herrero, Nature **556**, 43 (2018).
[124]G. Aromí, D. Aguilà, P. Gamez, F. Luis, and O. Roubeau, Chem. Soc. Rev. **41**, 537 (2012).
[125]D. Hsieh, D. Qian, L. Wray, Y. Xia, Y. S. Hor, R. J. Cava, and M. Z. Hasan, Nature **452**, 970 (2008).
[126]Z. Wang, Z. Liu, and F. Liu, Nat. Commun. **4**, 1471 (2013).
[127]Z. F. Wang, N. Su, and F. Liu, Nano Lett. **13**, 2842 (2013).
[128]L. Z. Zhang, Z. F. Wang, B. Huang, B. Cui, Z. Wang, S. X. Du, H.-J. Gao, and F. Liu, Nano Lett. **16**, 2072 (2016).
[129]C.-H. Hsu, Z.-Q. Huang, G. M. Macam, F.-C. Chuang, and L. Huang, Appl. Phys. Lett. **113**, 233301 (2018).
[130]S. Nakatsuji, N. Kiyohara, and T. Higo, Nature **527**, 212 (2015).
[131]C.-Z. Chang, W. Zhao, D. Y. Kim, H. Zhang, B. A. Assaf, D. Heiman, S.-C. Zhang, C. Liu, M. H. W. Chan, and J. S. Moodera, Nat. Mater. **14**, 473 (2015).